

Principal Component Analysis Based Broadband Hybrid Precoding for Millimeter-Wave Massive MIMO Systems

Yiwei Sun, Zhen Gao, *Member, IEEE*, Hua Wang, *Member, IEEE*, Byonghyo Shim, *Senior Member, IEEE*, Guan Gui, *Senior Member, IEEE*, Guoqiang Mao, *Fellow, IEEE*, and Fumiuki Adachi, *Life Fellow, IEEE*

arXiv:1903.09074v1 [cs.IT] 21 Mar 2019

Abstract—Hybrid analog-digital precoding is challenging for broadband millimeter-wave (mmWave) massive MIMO systems, since the analog precoder is frequency-flat but the mmWave channels are frequency-selective. In this paper, we propose a principal component analysis (PCA)-based broadband hybrid precoder/combiner design, where both the fully-connected array and partially-connected subarray (including the fixed and adaptive subarrays) are investigated. Specifically, we first design the hybrid precoder/combiner for fully-connected array and partially-connected subarray given the antenna grouping pattern based on PCA, whereby a low-dimensional frequency-flat precoder/combiner is extracted from the optimal high-dimensional frequency-selective precoder/combiner. Meanwhile, the near-optimality of our proposed PCA approach is theoretically proven. Moreover, for the adaptive subarray, a low-complexity shared agglomerative hierarchical clustering algorithm is proposed to group antennas for the further improvement of SE performance. Besides, we theoretically prove the proposed antenna grouping algorithm is only determined by the slow time-varying channel statistic information in the large antenna limit. Simulation results demonstrate the superiority of the proposed solution over state-of-the-art schemes in SE, energy efficiency (EE), and bit-error-rate performance. Our work reveals that the EE advantage of adaptive subarray over fully-connected array is obvious for both active and passive antennas, but the EE advantage of fixed subarray only holds for passive antennas.

Index Terms—Hybrid precoding, massive MIMO, OFDM, millimeter-wave, adaptive subarray, energy efficiency

I. INTRODUCTION

Millimeter-wave (mmWave) communication has been conceived to be a key enabling technology for the next-generation communications, since it can provide Gbps data rates by leveraging the large transmission bandwidth [3]–[6]. To combat the severe path loss in mmWave channels, a large number of antennas are usually employed at both the base stations (BS) and the mobile stations for beamforming

This paper was presented in part at the IEEE Global Communications Conference Workshop, December 2018 [1], [2].

Y. Sun, Z. Gao, and H. Wang are with School of Information and Electronics, Beijing Institute of Technology, Beijing, China (email: {sunyiwei, gaozhen16, wanghua}@bit.edu.cn). B. Shim is with Institute of New Media and Communications School of Electrical and Computer Engineering, Seoul National University, Seoul, Korea (email: bshim@korea.ac.kr). G. Gui is with College of Telecommunication and Information Engineering, Nanjing University of Posts and Telecommunications Nanjing, China (email: guiguan@njupt.edu.cn). G. Mao is with School of Computing and Communication, The University of Technology Sydney, Australia (email: g.mao@ieee.org). F. Adachi is with Dept. of Electrical and Communications Engineering Tohoku University, Sendai, Japan (email: adachi@ecei.tohoku.ac.jp).

[7], [8]. However, a large number of antennas could lead to severe hardware cost and power consumption if each antenna requires a radio frequency (RF) chain as in conventional fully-digital MIMO systems. To overcome this problem, hybrid MIMO has been emerging to trade off hardware cost with spectral efficiency (SE) and energy efficiency (EE) [9]–[13]. This tradeoff depends on the specific hybrid MIMO architecture, which includes the fully-connected array (FCA) and partially-connected subarray (PCS), and the latter can be further categorized into fixed subarray (FS) and adaptive subarray (AS) [14]. Nevertheless, how to design hybrid precoding over broadband channels can be challenging, as the RF precoding is frequency flat and has the constant-modulus constraint [7]. Therefore, it is of great importance to design an efficient broadband hybrid precoder/combiner for mmWave massive MIMO systems.

A. Related Work

Narrowband hybrid precoding has been investigated in [9], [10], [15]–[19]. Specifically, a compressive sensing (CS)-based hybrid precoding was proposed in [15], where the channel sparsity was exploited with the aid of orthogonal matching pursuit (OMP) algorithm. To reduce the computational complexity, a low-complexity CS-based beamspace hybrid precoding was developed in [16]. To improve the EE, an iterative analog precoding was designed for FS [17], but it failed to consider the digital precoding. Moreover, a constant envelope hybrid precoding scheme was proposed, where the hybrid precoding is designed under the per-antenna constant envelope constraints [9]. Additionally, the codebook-based scheme, the hybrid block diagonal scheme, and the heuristic scheme were respectively proposed in [10], [18], and [19] for multi-user MIMO. However, [9], [10], [15]–[19] only assumed the flat fading channels.

To effectively combat the time dispersive channels, several elegant broadband hybrid precoding solutions have been proposed in [20]–[23]. Most of them adopted OFDM so that the broadband frequency-selective fading channels were converted into multiple parallel narrowband flat fading channels. To be specific, a hybrid precoding scheme has been proposed in [20] to support single stream transmission in MIMO-OFDM system, where the optimal beam pair was exhaustively searched from a codebook predefined for FS. To reduce the computational complexity, an insightful broadband hybrid precoder based on limited-feedback codebook has been proposed for

fully-connected array (FCA) [21]. Moreover, by exploiting the channel correlation information among different subcarriers, a broadband hybrid precoding was proposed, where both FCA and PCS are investigated [22]. However, [21] did not consider the combiner design at the receiver, and [22] assumed the fully-digital array at the receiver. Note that in [22], although a greedy algorithm was proposed to group the antennas for AS, this method could suffer from the poor performance due to the unbalanced antenna grouping. Besides, by proving the dominant subspaces of frequency domain channel matrices at different subcarriers are equivalent, [23] has theoretically revealed the optimality of the frequency-flat precoding. However, this conclusion was based on the ideal sparse channels by assuming the discrete angles of arrival/departure (AoA/AoD), and the specific precoder/combiner solution was not explicitly provided.

B. Our Contributions

In this paper, we propose a general framework for broadband hybrid precoding for mmWave massive MIMO. To be specific, a near-optimal hybrid precoder and combiner are proposed for both FCA and PCS. In PCS, we not only investigate precoding scheme in FS, but also develop algorithm for AS antenna grouping. The contributions of this paper are summarized as follows:

- **Near-optimal PCA-based analog precoder and combiner design.** Based on the PCA, the low-dimensional signal space of frequency-flat precoder can be abstracted from the high-dimensional signal space of optimal frequency-selective precoder with small SE performance loss. Moreover, to minimize the mean square error between transmit and receive symbols, a weighted PCA is proposed to obtain the analog combiner for improved BER performance. Further, we show the optimality of the proposed PCA-based hybrid precoding design theoretically and demonstrate by simulations.
- **Low-complexity antenna grouping for AS based on shared-AHC algorithm.** We formulate the antenna grouping problem for AS as the clustering problem in machine learning. To avoid the prohibitively high complexity of optimal exhaustive search approach, we propose a low-complexity shared-AHC algorithm. Moreover, we prove that the shared-AHC relay on the direction of multipaths with large gains and thus does not have to change rapidly with the time-varying channel. Simulation results confirm that the proposed shared-AHC algorithm achieves better SE and EE performance than existing schemes. Additionally, simulations indicate the complexity varying with antenna numbers and channel realizations, and further confirm the SE performance of unchanged AS coincide with changed AS in time-varying channels.
- **EE performance analysis in practical passive/active antennas.** Antenna architectures are different for passive and active antennas, which leads to the different numbers of power-consuming electronic elements (e.g., power amplifiers). EE analysis in prior work usually assumes the simplified antenna model without distinguishing passive/active antennas. By contrast, we consider

the practical passive/active antennas for EE performance analysis. Our work reveals that EE advantage of FS over FCA is obvious for passive antennas, but this advantage gap decreases for active antennas. Meanwhile, AS has the overwhelming advantage for both active and passive antennas.

The rest of this paper is organized as follows. We introduce the system model in Section II. Then, we propose PCA-based hybrid precoder and combiner for FCA in Section III. Moreover, we extend the precoding design to PCS in Section IV, whereby PCA-based precoding scheme in FS and shared-AHC based antenna grouping scheme in AS are discussed. In Section V, we evaluate the system performance, including the SE, BER and EE performance of the proposed PCA-based precoding scheme, the computational complexity and slow time-varying feature of the shared-AHC based AS antenna grouping algorithm. Finally, we conclude the paper in Section VII.

Notations: Following notations are used throughout this paper. \mathbf{A} is a matrix, \mathbf{a} is a vector, a is a scalar, and \mathcal{A} is a set. Conjugate transpose and transpose of \mathbf{A} are \mathbf{A}^H and \mathbf{A}^T , respectively. The (i, j) th entry of \mathbf{A} is $[\mathbf{A}]_{i,j}$, $[\mathbf{A}]_{i,:}$ ($[\mathbf{A}]_{:,j}$) denotes the i th row (j th column) of \mathbf{A} , sub-matrix $[\mathbf{A}]_{i_1:i_2,:}$ ($[\mathbf{A}]_{:,j_1:j_2}$) consists of the i_1 th to i_2 th rows (j_1 th to j_2 th columns) of \mathbf{A} , and sub-matrix $[\mathbf{A}]_{i_1:i_2,j_1:j_2}$ consists of the i_1 th to i_2 th rows and j_1 th to j_2 th columns of \mathbf{A} . Frobenius norm and ℓ_2 -norm are denoted by $\|\cdot\|_F$ and $\|\cdot\|_2$, respectively. $\det(\mathbf{A})$ is the determinant of a square matrix \mathbf{A} . $\text{card}(\mathcal{A})$ is the cardinality of a set \mathcal{A} . $|a|$ is the modulus of a number a . $\angle(a)$ denotes the phase of a complex number a . \otimes represents the Kronecker product. Subtraction between sets \mathcal{A} and \mathcal{B} is defined as $\mathcal{A} \setminus \mathcal{B} = \{x | x \in \mathcal{A} \& x \notin \mathcal{B}\}$. Especially, \mathbf{I}_N denotes an identity matrix with size $N \times N$. The i th largest singular value of a matrix \mathbf{A} is defined as $\lambda_i(\mathbf{A})$. Additionally, $\text{blkdiag}(\mathbf{a}_1, \dots, \mathbf{a}_K)$ is a block diagonal matrix with \mathbf{a}_i ($1 \leq i \leq K$) on its diagonal blocks. Finally, $\Re\{\mathbf{A}\}$ means to keep the real part of a complex matrix \mathbf{A} .

II. SYSTEM MODEL

We consider an mmWave massive 3-dimensional (3D) MIMO system, where both the BS and the user employ the uniform planar array (UPA), and OFDM is adopted to combat the frequency-selective fading channels. The BS is equipped with $N_t = N_t^v \times N_t^h$ antennas and $N_t^{\text{RF}} \ll N_t$ RF chains, where N_t^v and N_t^h are the numbers of vertical and horizontal transmit antennas, respectively. The user is equipped with $N_r = N_r^v \times N_r^h$ antennas and $N_r^{\text{RF}} \ll N_r$ RF chains, where N_r^v and N_r^h are the numbers of vertical and horizontal receive antennas, respectively. In the downlink, the received symbols of the k th subcarrier at the user are [15]

$$\mathbf{r}[k] = (\mathbf{W}_{\text{RF}} \mathbf{W}_{\text{BB}}[k])^H (\mathbf{H}[k] \mathbf{F}_{\text{RF}} \mathbf{F}_{\text{BB}}[k] \mathbf{x}[k] + \mathbf{n}[k]), \quad (1)$$

where $1 \leq k \leq K$ with K being the number of subcarriers, $\mathbf{F}_{\text{BB}}[k] \in \mathbb{C}^{N_t^{\text{RF}} \times N_s}$, $\mathbf{F}_{\text{RF}} \in \mathbb{C}^{N_t \times N_r^{\text{RF}}}$, $\mathbf{W}_{\text{BB}}[k] \in \mathbb{C}^{N_r^{\text{RF}} \times N_s}$, $\mathbf{W}_{\text{RF}} \in \mathbb{C}^{N_r \times N_r^{\text{RF}}}$, $\mathbf{H}[k] \in \mathbb{C}^{N_r \times N_t}$, $\mathbf{x}[k] \in \mathbb{C}^{N_s \times 1}$, and $\mathbf{n}[k] \in \mathbb{C}^{N_r \times 1}$ are the digital precoder, analog precoder, digital combiner, analog combiner, channel matrix,

transmitted signal, and noise associated with the k th subcarrier, respectively, and N_s is the number of data streams. $\mathbf{n}[k] \sim \mathcal{CN}(0, \sigma_n^2 \mathbf{I}_{N_r})$ and $\mathbf{x}[k]$ satisfies $\mathbb{E}[\mathbf{x}[k]\mathbf{x}^H[k]] = \mathbf{I}_{N_s}$. The frequency-domain channel $\mathbf{H}[k]$ can be expressed as $\mathbf{H}[k] = \sum_{d=0}^{D-1} \mathbf{H}_d[d] e^{-j\frac{2\pi k}{K}d}$, where D is the maximum delay spread of the discretized channels, and $\mathbf{H}_d[d] \in \mathbb{C}^{N_r \times N_t}$ is the delay- d channel matrix. We consider the clustered channel model [15], where the channel comprises N_{cl} clusters of multipaths with N_{ray} rays in each cluster. Thus, the delay- d channel matrix can be written as

$$\mathbf{H}_d[d] = \sum_{i=1}^{N_{\text{cl}}} \sum_{l=1}^{N_{\text{ray}}} p_{i,l}^d[d] \mathbf{a}_r(\phi_{i,l}^r, \theta_{i,l}^r) \mathbf{a}_t^H(\phi_{i,l}^t, \theta_{i,l}^t), \quad (2)$$

where $p_{i,l}^d[d] = \sqrt{N_t N_r / (N_{\text{cl}} N_{\text{ray}})} \alpha_{i,l} p(dT_s - \tau_{i,l})$ is the delay-domain channel coefficient, $\tau_{i,l}$, $\alpha_{i,l}$, and $p(\tau)$ are the delay, the complex path gain, and the pulse shaping filter for T_s -spaced signaling, respectively. Thus the relationship between the frequency-domain channel coefficient and the delay-domain channel coefficient is $p_{i,l}[k] = \sum_{d=0}^{D-1} p_{i,l}^d[d] \exp(-j2\pi kd/K)$. In (2), $\mathbf{a}_t(\phi_{i,l}^t, \theta_{i,l}^t)$ and $\mathbf{a}_r(\phi_{i,l}^r, \theta_{i,l}^r)$ are the steering vectors of the l th path in the i th cluster at the transmitter and receiver, respectively. In the steering vectors, $\phi_{i,l}^t$ and $\theta_{i,l}^t$ are the azimuth and elevation angles of the l th ray in the i th cluster for AoDs, and $\phi_{i,l}^r$ and $\theta_{i,l}^r$ are the azimuth and elevation angles of the l th ray in the i th cluster for AoAs. Taking AoD for illustration, the vertical and horizontal steering vectors for the UPA at the BS can be expressed as $\mathbf{e}_t^v(\Omega_{i,l}^v) = [1 \ e^{-j2\pi\Omega_{i,l}^v} \ \dots \ e^{-j2\pi(N_t^v-1)\Omega_{i,l}^v}]^T / \sqrt{N_t^v}$ and $\mathbf{e}_t^h(\Omega_{i,l}^h) = [1 \ e^{-j2\pi\Omega_{i,l}^h} \ \dots \ e^{-j2\pi(N_t^h-1)\Omega_{i,l}^h}]^T / \sqrt{N_t^h}$, where $\Omega_{i,l}^h = d_h \sin(\theta_{i,l}^t) \sin(\phi_{i,l}^t) / \lambda$ and $\Omega_{i,l}^v = d_v \cos(\theta_{i,l}^t) / \lambda$, λ is the carrier wavelength, and d_v , d_h are the distances between adjacent antenna elements in vertical and horizontal direction, respectively [8]. Thus the steering vector of the l th ray in the i th cluster for AoD is $\mathbf{a}_t(\phi_{i,l}^t, \theta_{i,l}^t) = \mathbf{e}_t^v(\Omega_{i,l}^v) \otimes \mathbf{e}_t^h(\Omega_{i,l}^h)$. Similarly, the receive steering vectors are $\mathbf{a}_r(\phi_{i,l}^r, \theta_{i,l}^r) = \frac{1}{\sqrt{N_r}} [1 \ \dots \ e^{-j2\pi(m\Psi_{i,l}^h+n\Psi_{i,l}^v)} \ \dots \ e^{-j2\pi((N_r^h-1)\Psi_{i,l}^h+(N_r^v-1)\Psi_{i,l}^v)}]^T$, for $1 \leq i \leq N_{\text{cl}}$, $1 \leq l \leq N_{\text{ray}}$, where $\Psi_{i,l}^h = d_h \sin(\theta_{i,l}^r) \sin(\phi_{i,l}^r) / \lambda$ and $\Psi_{i,l}^v = d_v \cos(\theta_{i,l}^r) / \lambda$.

The achievable SE for the mmWave MIMO-OFDM system can be expressed as [21]

$$R = \frac{1}{K} \sum_{k=1}^K \log_2 (\det(\mathbf{I} + \frac{1}{N_s} \mathbf{R}_n^{-1}[k] \mathbf{W}_{\text{BB}}^H[k] \mathbf{W}_{\text{RF}}^H \mathbf{H}[k] \mathbf{F}_{\text{RF}} \mathbf{F}_{\text{BB}}[k] \mathbf{F}_{\text{BB}}^H[k] \mathbf{F}_{\text{RF}}^H \mathbf{H}^H[k] \mathbf{W}_{\text{RF}} \mathbf{W}_{\text{BB}}[k])), \quad (3)$$

where $\mathbf{R}_n[k] = \sigma_n^2 \mathbf{W}_{\text{BB}}^H[k] \mathbf{W}_{\text{RF}}^H \mathbf{W}_{\text{RF}} \mathbf{W}_{\text{BB}}[k]$. It is worthy to point out that our work is distinctly different from the previous work [22] with the hybrid precoder considered at the transmitter but fully-digital combiner assumed at the receiver. In this paper, we consider the hybrid MIMO architecture at both the transmitter and receiver. Our goal is to design the hybrid precoder and combiner that maximizes the SE. Since the sum rate R is a function of variables $(\mathbf{F}_{\text{RF}}, \{\mathbf{F}_{\text{BB}}[k]\}_{k=1}^K, \mathbf{W}_{\text{RF}}, \{\mathbf{W}_{\text{BB}}[k]\}_{k=1}^K)$, it is computationally inefficient to jointly optimize the sum rate. To combat the

problem, we propose an approach to decouple the design of precoder and combiner to solve this intractable problem.

III. PCA-BASED PRECODER/COMBINER FOR FCA

This section will discuss the design of the precoder/combiner for hybrid mmWave MIMO with FCA. Our goal is to design the optimal frequency-flat RF precoder (combiner) based on the optimal fully-digital frequency-selective precoder (combiner).

A. PCA-Based Precoder Design at Transmitter

We first design the digital precoder by fixing the RF precoder. Specifically, we design the precoder that maximizes the rate of the signalling. The corresponding optimization problem is

$$\begin{aligned} \max_{\mathbf{F}_{\text{RF}}, \{\mathbf{F}_{\text{BB}}[k]\}_{k=1}^K} & \sum_{k=1}^K \log_2 (\det(\mathbf{I}_{N_r} + \frac{1}{\sigma_n^2} \mathbf{H}[k] \mathbf{F}_{\text{RF}} \mathbf{F}_{\text{BB}}[k] \mathbf{F}_{\text{BB}}^H[k] \mathbf{F}_{\text{RF}}^H \mathbf{H}^H[k])) \\ \text{s.t. } & \mathbf{F}_{\text{RF}} \in \mathcal{F}_{\text{RF}}, \sum_{k=1}^K \|\mathbf{F}_{\text{RF}} \mathbf{F}_{\text{BB}}[k]\|_F^2 = KN_s, \end{aligned} \quad (4)$$

where \mathcal{F}_{RF} is a set of feasible RF precoder satisfying constant-modulus constraint. The joint optimization of \mathbf{F}_{RF} and $\{\mathbf{F}_{\text{BB}}[k]\}_{k=1}^K$ in (4) is very difficult due to the coupling between the baseband and RF precoders [21]. Therefore, we design \mathbf{F}_{RF} and $\{\mathbf{F}_{\text{BB}}[k]\}_{k=1}^K$ separately. We consider $\tilde{\mathbf{F}}_{\text{BB}}[k] = (\mathbf{F}_{\text{RF}}^H \mathbf{F}_{\text{RF}})^{\frac{1}{2}} \mathbf{F}_{\text{BB}}[k]$ to be the equivalent baseband precoder. Then the optimization problem (4) is equivalent to

$$\begin{aligned} \max_{\mathbf{F}_{\text{RF}}, \{\tilde{\mathbf{F}}_{\text{BB}}[k]\}_{k=1}^K} & \sum_{k=1}^K \log_2 (\det(\mathbf{I}_{N_r} + \frac{1}{\sigma_n^2} \mathbf{H}[k] \mathbf{F}_{\text{RF}} (\mathbf{F}_{\text{RF}}^H \mathbf{F}_{\text{RF}})^{-\frac{1}{2}} \tilde{\mathbf{F}}_{\text{BB}}[k] \tilde{\mathbf{F}}_{\text{BB}}^H[k] (\mathbf{F}_{\text{RF}}^H \mathbf{F}_{\text{RF}})^{-\frac{1}{2}} \mathbf{H}^H[k])) \\ \text{s.t. } & \mathbf{F}_{\text{RF}} \in \mathcal{F}_{\text{RF}}, \sum_{k=1}^K \|\tilde{\mathbf{F}}_{\text{BB}}[k]\|_F^2 = KN_s. \end{aligned} \quad (5)$$

In solving the problem (5), we first consider the optimal solution of $\{\tilde{\mathbf{F}}_{\text{BB}}[k]\}_{k=1}^K$. Specifically, the singular value decomposition (SVD) of $\mathbf{H}[k]$ associated with the k th subcarrier is

$$\mathbf{H}[k] = \mathbf{U}[k] \mathbf{\Sigma}[k] \mathbf{V}^H[k], \quad (6)$$

and the SVD of the matrix $\mathbf{\Sigma}[k] \mathbf{V}^H[k] \mathbf{F}_{\text{RF}} (\mathbf{F}_{\text{RF}}^H \mathbf{F}_{\text{RF}})^{-1/2} = \tilde{\mathbf{U}}[k] \tilde{\mathbf{\Sigma}}[k] \tilde{\mathbf{V}}^H[k]$. Therefore, the equivalent baseband precoder $\tilde{\mathbf{F}}_{\text{BB}}[k] = [\tilde{\mathbf{V}}[k]]_{:,1:N_s} \mathbf{\Lambda}[k]$, and thus the optimal baseband precoder $\mathbf{F}_{\text{BB}}[k]$ can be expressed as

$$\mathbf{F}_{\text{BB}}[k] = (\mathbf{F}_{\text{RF}}^H \mathbf{F}_{\text{RF}})^{-\frac{1}{2}} \tilde{\mathbf{F}}_{\text{BB}}[k] = (\mathbf{F}_{\text{RF}}^H \mathbf{F}_{\text{RF}})^{-\frac{1}{2}} [\tilde{\mathbf{V}}[k]]_{:,1:N_s} \mathbf{\Lambda}[k], \quad (7)$$

where $\mathbf{\Lambda}[k] \in \mathbb{C}^{N_s \times N_s}$ is a water-filling solution matrix, i.e.,

$$[\mathbf{\Lambda}[k]]_{i,i}^2 = (\mu - \frac{N_s}{[\tilde{\mathbf{V}}[k]]_{i,i}^2})^+, \quad 1 \leq i \leq N_s, 1 \leq k \leq K, \quad (8)$$

where the function $(\cdot)^+$ denotes $(a)^+ = a$ if $a > 0$, otherwise $(a)^+ = 0$, and μ satisfies $\sum_{k=1}^K \sum_{i=1}^{N_s} (\mu - N_s / [\tilde{\mathbf{V}}[k]]_{i,i}^2)^+ = KN_s$. Then the joint optimization of \mathbf{F}_{RF} and $\{\mathbf{F}_{\text{BB}}[k]\}_{k=1}^K$ is reduced to the optimization of \mathbf{F}_{RF} in (5).

Algorithm 1 PCA-based RF Precoder Design.

Input: Optimal precoder $\{\mathbf{F}_{\text{opt}}[k]\}_{k=1}^K$, the number of RF chains N_t^{RF} , and the number of antennas N_t .

Output: RF precoder \mathbf{F}_{RF} .

- 1: $\mathbf{F} = [\mathbf{F}_{\text{opt}}[1] \ \mathbf{F}_{\text{opt}}[2] \ \cdots \ \mathbf{F}_{\text{opt}}[K]]$
- 2: Apply SVD to \mathbf{F} , i.e., $\mathbf{F} = \mathbf{U}_F \boldsymbol{\Sigma}_F \mathbf{V}_F^H$, where \mathbf{U}_F corresponds to the principal components
- 3: $[\mathbf{F}_{\text{RF}}]_{i,j} = \frac{1}{\sqrt{N_t}} e^{j\angle([\mathbf{U}_F]_{i,j})}$

We first define the optimal fully-digital precoder $\mathbf{F}_{\text{opt}}[k] = [\mathbf{V}[k]]_{:,1:N_s}$ for $1 \leq k \leq K$. The optimization problem in (4) can have transformation shown in Lemma 1.

Lemma 1. *Optimization problem in (4) can be approximately written as*

$$\max_{\mathbf{F}_{\text{RF}}} \sum_{k=1}^K \|\mathbf{F}_{\text{opt}}^H[k] \mathbf{F}_{\text{RF}} \mathbf{F}_{\text{BB}}[k]\|_F^2 \quad (9)$$

s.t. $\mathbf{F}_{\text{RF}} \in \mathcal{F}_{\text{RF}}$.

Especially, optimization problem (4) is equal to (9) when the following requirements are reached:

- 1) Hybrid precoder $\mathbf{F}_{\text{RF}} \mathbf{F}_{\text{BB}}[k]$ can be sufficiently “close” to the optimal fully-digital precoder $\mathbf{F}_{\text{opt}}[k] = \mathbf{F}_{\text{RF}} \mathbf{F}_{\text{BB}}[k]$.
- 2) The signal-to-noise ratio (SNR) is high.

Proof. See Appendix A. \square

In [23], it has been shown that the frequency domain MIMO channel matrices $\{\mathbf{H}[k]\}_{k=1}^K$ have the same column space and row space. Meanwhile, the frequency-flat RF precoder \mathbf{F}_{RF} remains unchanged for all subcarriers. So the RF precoder can be regarded as a representation of such a column space. This observation motivates us to design the RF precoder by leveraging the PCA [26]. Specifically, we regard the matrix $\mathbf{F} = [\mathbf{F}_{\text{opt}}[1] \ \mathbf{F}_{\text{opt}}[2] \ \cdots \ \mathbf{F}_{\text{opt}}[K]]$ consisting of the optimal precoders of all subcarriers as the data set in the PCA problem. Additionally, to achieve the stable solution with low complexity for PCA, SVD is applied to the data set matrix \mathbf{F} [26]. The process is shown in the following proposition.

Proposition 1. *Considering $\mathbf{F} = [\mathbf{F}_{\text{opt}}[1] \ \mathbf{F}_{\text{opt}}[2] \ \cdots \ \mathbf{F}_{\text{opt}}[K]]$ and its SVD $\mathbf{F} = \mathbf{U}_F \boldsymbol{\Sigma}_F \mathbf{V}_F^H$, the solution to (9) can be expressed as $\mathbf{F}_{\text{RF}} = [\mathbf{U}_F]_{:,1:N_t^{\text{RF}}} \mathbf{R}_t$, where $\mathbf{R}_t \in \mathbb{C}^{N_t^{\text{RF}} \times N_t^{\text{RF}}}$ is an arbitrary full rank matrix.*

Proof. See Appendix B. \square

According to Proposition 1, we can obtain the principal components constituting the optimal RF precoder using PCA. Moreover, we will design the full-rank matrix \mathbf{R}_t to meet the requirement of constant-modulus constraint for RF precoder. Specifically, by taking the constant-modulus constraint of RF precoder into account, we can design the RF precoder by solving

$$\mathbf{F}_{\text{RF}} = \arg \min_{\|\mathbf{X}[k]\|_2 = 1/\sqrt{N_t}} \|\mathbf{X} - [\mathbf{U}_F]_{:,1:N_t^{\text{RF}}} \|^2_F. \quad (10)$$

When the constant-modulus constraint is employed, the set of possible \mathbf{F}_{RF} is actually a hypersphere in the space of $\mathbb{C}^{N_t \times N_t^{\text{RF}}}$, and $[\mathbf{U}_F]_{:,1:N_t^{\text{RF}}}$ is a known point in the space of $\mathbb{C}^{N_t \times N_t^{\text{RF}}}$. Therefore, the optimization problem in (10) is essentially to search a solution in the hypersphere according to the distance minimization criterion from a fix point $[\mathbf{U}_F]_{:,1:N_t^{\text{RF}}}$. Naturally, the solution is the point on this hypersphere sharing the same direction of the known point. In other words, the solution is given by $[\mathbf{F}_{\text{RF}}]_{i,j} = 1/\sqrt{N_t} e^{j\angle([\mathbf{U}_F]_{i,j})}$. Therefore, the matrix $\mathbf{R}_t = ([\mathbf{U}_F]_{:,1:N_t^{\text{RF}}} [\mathbf{U}_F]_{:,1:N_t^{\text{RF}}}^H)^{-1} [\mathbf{U}_F]_{:,1:N_t^{\text{RF}}}^H \mathbf{F}_{\text{RF}}$. The specific RF precoder design can be summarized in Algorithm 1. Note that our method has essential difference with [22]. The frequency flat component (RF precoder) of [22] is estimated by the eigenvectors of channel covariance matrix. While in our proposed scheme, the frequency flat component (RF precoder) is estimated by the common basis of row space of channel matrices in all subcarriers, i.e. the eigenvectors of the covariance of the row space of channel matrices under all subcarriers. Apparently, the covariance of the row space of channel matrices is **not** the channel covariance matrix. Thus, our proposed PCA-based precoding scheme portrays the frequency flat component of the frequency selective channel in different perspective.

When the quantization of phase shifters is considered [27], we assume that the quantization bits are Q . Therefore, the phase shifters can only be chosen from the following quantized phase set $\mathcal{Q} = \{0, \frac{2\pi}{2^Q}, \dots, \frac{2\pi(2^Q-1)}{2^Q}\}$. Specifically, after obtaining the RF precoder \mathbf{F}_{RF} , the quantization process can be realized by searching for the minimum Euclidean distance between $\angle([\mathbf{F}_{\text{RF}}]_{i,j})$ and quantized phase from \mathcal{Q} .

B. PCA-Based Combiner Design at Receiver

In this subsection, we seek to design the hybrid combiner to minimize the mean-square-error (MSE) between the received signal and the transmitted signal under the assumption that \mathbf{F}_{RF} and $\{\mathbf{F}_{\text{BB}}[k]\}_{k=1}^K$ are fixed [15]. Specifically, the optimal fully-digital minimum mean square error (MMSE) combiner can be expressed as

$$\begin{aligned} \mathbf{W}_{\text{opt}}^H[k] = & \mathbf{W}_{\text{MMSE}}^H[k] = \frac{1}{N_s} \mathbf{F}_{\text{BB}}^H[k] \mathbf{F}_{\text{RF}}^H \mathbf{H}^H[k] (\sigma_n^2 \mathbf{I}_{N_r})^{-1} \\ & + \frac{1}{N_s} \mathbf{H}[k] \mathbf{F}_{\text{RF}} \mathbf{F}_{\text{BB}}[k] \mathbf{F}_{\text{BB}}^H[k] \mathbf{F}_{\text{RF}}^H \mathbf{H}^H[k], \end{aligned} \quad (11)$$

for $1 \leq k \leq K$. Denoting the signal at the receive antenna as $\mathbf{y}[k] \in \mathbb{C}^{N_r \times 1}$ ($1 \leq k \leq K$), the combiner design can be formulated as the following optimization problem:

$$\begin{aligned} \min_{\mathbf{W}_{\text{RF}}, \{\mathbf{W}_{\text{BB}}[k]\}_{k=1}^K} & \sum_{k=1}^K \mathbb{E}[\|\mathbf{x}[k] - \mathbf{W}_{\text{BB}}^H[k] \mathbf{W}_{\text{RF}}^H \mathbf{y}[k]\|_2^2] \\ \text{s.t. } & \mathbf{W}_{\text{RF}} \in \mathcal{W}_{\text{RF}}, \end{aligned} \quad (12)$$

where \mathcal{W}_{RF} is a set of feasible RF combiner satisfying constant-modulus constraint. Note that if the constant-modulus constraint in (12) is removed, the solution to the problem (12) becomes equivalent to the optimal fully-digital MMSE

Algorithm 2 Weighted PCA-based RF Combiner Design.

Input: Optimal combiners $\{\mathbf{W}_{\text{opt}}[k]\}_{k=1}^K$, covariance matrices of the received signals $\{\mathbb{E}[\mathbf{y}[k]\mathbf{y}^H[k]]^{1/2}\}_{k=1}^K$, the number of RF chains N_r^{RF} , and the number of antennas N_r .

Output: RF combiner \mathbf{W}_{RF} .

- 1: $\mathbf{A}[k] = \mathbb{E}[\mathbf{y}[k]\mathbf{y}^H[k]]^{1/2}\mathbf{W}_{\text{opt}}[k]$ for $1 \leq k \leq K$
- 2: $\mathbf{W} = [\mathbf{A}[1] \ \mathbf{A}[2] \ \dots \ \mathbf{A}[K]]$
- 3: Apply SVD to \mathbf{W} , i.e., $\mathbf{W} = \mathbf{U}_W \mathbf{\Sigma}_W \mathbf{V}_W^H$, where \mathbf{U}_W corresponds to the principal components
- 4: $[\mathbf{W}_{\text{RF}}]_{i,j} = \frac{1}{\sqrt{N_r}} e^{j\angle([\mathbf{U}_W]_{i,j})}$

combiner in (11). Note that the objective function in (12) can be further expressed as

$$\begin{aligned} & \sum_{k=1}^K \mathbb{E}[\|\mathbf{x}[k] - \mathbf{W}_{\text{BB}}^H[k]\mathbf{W}_{\text{RF}}^H\mathbf{y}[k]\|_2^2] \\ &= \sum_{k=1}^K \text{Tr}(\mathbb{E}[\mathbf{x}[k]\mathbf{x}^H[k]]) - 2 \sum_{k=1}^K \mathcal{R}\{\text{Tr}(\mathbb{E}[\mathbf{x}[k]\mathbf{y}^H[k]]\mathbf{W}_{\text{RF}}\mathbf{W}_{\text{BB}}[k])\} \\ & \quad + \text{Tr}(\mathbf{W}_{\text{BB}}^H[k]\mathbf{W}_{\text{RF}}^H\mathbb{E}[\mathbf{y}[k]\mathbf{y}^H[k]]\mathbf{W}_{\text{RF}}\mathbf{W}_{\text{BB}}[k]). \end{aligned} \quad (13)$$

Since the optimization variables in (12) are \mathbf{W}_{RF} and $\{\mathbf{W}_{\text{BB}}[k]\}_{k=1}^K$, terms unrelated to \mathbf{W}_{RF} and $\{\mathbf{W}_{\text{BB}}[k]\}_{k=1}^K$ will not affect the solution. Thus we add the independent term $\sum_{k=1}^K \text{Tr}(\mathbf{W}_{\text{opt}}^H[k]\mathbb{E}[\mathbf{y}[k]\mathbf{y}^H[k]]\mathbf{W}_{\text{opt}}[k]) - \sum_{k=1}^K \text{Tr}(\mathbb{E}[\mathbf{x}[k]\mathbf{x}^H[k]])$ to the objective function (13). Thus, the optimization problem (12) can be rewritten as

$$\sum_{k=1}^K \|\mathbb{E}[\mathbf{y}[k]\mathbf{y}^H[k]]^{1/2}(\mathbf{W}_{\text{opt}}[k] - \mathbf{W}_{\text{RF}}\mathbf{W}_{\text{BB}}[k])\|_F^2, \quad (14)$$

s.t. $\mathbf{W}_{\text{RF}} \in \mathcal{W}_{\text{RF}}$,

where $\mathbb{E}[\mathbf{y}[k]\mathbf{y}^H[k]] = \frac{1}{N_s} \mathbf{H}[k] \mathbf{F}_{\text{RF}} \mathbf{F}_{\text{BB}}[k] \mathbf{F}_{\text{BB}}^H[k] \mathbf{F}_{\text{RF}}^H \mathbf{H}^H[k] + \sigma_n^2 \mathbf{I}_{N_r}$. In practical scenario, it is easier to obtain $\mathbb{E}[\mathbf{y}[k]\mathbf{y}^H[k]]$ using the received signal $\mathbf{y}[k]$ instead of the equation. Here we use the equation only for the convenience of mathematical derivation. It is very difficult to jointly obtain \mathbf{W}_{RF} and $\{\mathbf{W}_{\text{BB}}[k]\}_{k=1}^K$ due to the coupling between baseband and RF combiner. Therefore, we design \mathbf{W}_{RF} and $\{\mathbf{W}_{\text{BB}}[k]\}_{k=1}^K$ separately. We fix the RF combiner \mathbf{W}_{RF} and consider weighted LS estimation of baseband combiner

$$\mathbf{W}_{\text{BB}}[k] = (\mathbf{W}_{\text{RF}}^H \mathbb{E}[\mathbf{y}[k]\mathbf{y}^H[k]] \mathbf{W}_{\text{RF}})^{-1} \mathbf{W}_{\text{RF}}^H \mathbb{E}[\mathbf{y}[k]\mathbf{y}^H[k]] \mathbf{W}_{\text{opt}}[k] \quad (15)$$

To design RF combiner \mathbf{W}_{RF} , a frequency flat combiner needs to be extracted from the frequency selective combiner $\{\mathbf{W}_{\text{opt}}[k]\}_{k=1}^K$. This can be obtained using weighted PCA. The process is shown in Proposition 2.

Proposition 2. Considering $\mathbf{W} = [\mathbb{E}[\mathbf{y}[1]\mathbf{y}^H[1]]^{1/2}\mathbf{W}_{\text{opt}}[1] \ \dots \ \mathbb{E}[\mathbf{y}[K]\mathbf{y}^H[K]]^{1/2}\mathbf{W}_{\text{opt}}[K]]$ and its SVD $\mathbf{W} = \mathbf{U}_W \mathbf{\Sigma}_W \mathbf{V}_W^H$, the solution to (14) can be written as $\mathbf{W}_{\text{RF}} = [\mathbf{U}_W]_{:,1:N_r^{\text{RF}}} \mathbf{R}_r$, where $\mathbf{R}_r \in \mathbb{C}^{N_r^{\text{RF}} \times N_r^{\text{RF}}}$ is an arbitrary full rank matrix.

Proof. See Appendix C. □

Algorithm 3 Baseband Combiner Design.

Input: Optimal combiners $\{\mathbf{W}_{\text{opt}}[k]\}_{k=1}^K$, RF combiner \mathbf{W}_{RF} , RF precoder \mathbf{F}_{RF} , baseband precoders $\{\mathbf{F}_{\text{BB}}[k]\}_{k=1}^K$, channel matrices $\{\mathbf{H}[k]\}_{k=1}^K$, and expectation of the received signal $\{\mathbb{E}[\mathbf{y}[k]\mathbf{y}^H[k]]\}_{k=1}^K$.

Output: Baseband combiners $\{\mathbf{W}_{\text{BB}}[k]\}_{k=1}^K$.

- 1: **for** $k = 1 : K$ **do**
- 2: $\mathbf{A} = (\mathbf{W}_{\text{RF}}^H \mathbb{E}[\mathbf{y}[k]\mathbf{y}^H[k]] \mathbf{W}_{\text{RF}})^{-1}$
- 3: $\mathbf{W}_{\text{BB}}[k] = \mathbf{A} \mathbf{W}_{\text{RF}}^H \mathbb{E}[\mathbf{y}[k]\mathbf{y}^H[k]] \mathbf{W}_{\text{opt}}[k]$
- 4: $\mathbf{\Lambda}_{\text{eq}} = \text{diag}\{\mathbf{W}_{\text{BB}}^H[k] \mathbf{W}_{\text{RF}}^H \mathbf{H}[k] \mathbf{F}_{\text{RF}} \mathbf{F}_{\text{BB}}[k]\}^{-1}$
- 5: $\mathbf{W}_{\text{BB}}[k] = \mathbf{W}_{\text{BB}}[k] \mathbf{\Lambda}_{\text{eq}}$
- 6: **end for**

The design of RF combiner can be extended from that of the RF precoder, where the weight $\mathbb{E}[\mathbf{y}[k]\mathbf{y}^H[k]]$ is designed based on the MMSE criterion. The RF combiner design is provided in Algorithm 2. When the quantization of phase shifters is considered, the entries of $\angle([\mathbf{W}_{\text{RF}}]_{i,j})$ are substituted by the phase in Q bits quantization phase set \mathcal{Q} with minimum Euclidean distance.

It is worth pointing out that baseband combiner $\{\mathbf{W}_{\text{BB}}[k]\}_{k=1}^K$ should also have the function of equalizer. Otherwise, it may cause fatal error in BER performance. The detailed design of $\{\mathbf{W}_{\text{BB}}[k]\}_{k=1}^K$ can be summarized in Algorithm 3.

IV. HYBRID PRECODER/COMBINER DESIGN FOR PCS

In this section, we further discuss the hybrid precoders and combiners for PCS, in which only a subset of antennas is connected to a concerning RF chain. We first discuss the precoding scheme under a given subarray (FS). Then, we further improve the antenna grouping to obtain better SE performance.

A. Hybrid Precoder/Combiner Design for FS

At the transmitter, there are N_t antennas and N_t^{RF} RF chains. For simplicity, we consider the numbers of antennas for different RF chains are identical, and the cardinality of each subset for every antenna group is $N_t^{\text{sub}} = N_t/N_t^{\text{RF}}$. We define the set of antenna indexes as $\{1, \dots, N_t\}$, and \mathcal{S}_r as the subset of the antennas associated with the r th RF chain, where $\mathcal{S}_r = \{(r-1)N_t^{\text{sub}} + 1, \dots, rN_t^{\text{sub}}\}$, for $1 \leq r \leq N_t^{\text{RF}}$. For the FS, the analog precoder \mathbf{F}_{RF} can be written as a block diagonal matrix $\mathbf{F}_{\text{RF}} = \text{blkdiag}(\mathbf{f}_{\text{RF},\mathcal{S}_1}, \dots, \mathbf{f}_{\text{RF},\mathcal{S}_{N_t^{\text{RF}}}})$, where $\mathbf{f}_{\text{RF},\mathcal{S}_r} \in \mathbb{C}^{N_t^{\text{sub}} \times 1}$ is the analog beamforming vector associated with the r th subarray for the r th RF chain. Specifically, similar to the precoder design for FCA, we consider the equivalent RF precoder $\bar{\mathbf{F}}_{\text{RF}} = \mathbf{F}_{\text{RF}}(\mathbf{F}_{\text{RF}}^H \mathbf{F}_{\text{RF}})^{-1/2}$, which can be expressed as

$$\bar{\mathbf{F}}_{\text{RF}} = \text{blkdiag}\left(\frac{\mathbf{f}_{\text{RF},\mathcal{S}_1}}{\|\mathbf{f}_{\text{RF},\mathcal{S}_1}\|_2}, \dots, \frac{\mathbf{f}_{\text{RF},\mathcal{S}_{N_t^{\text{RF}}}}}{\|\mathbf{f}_{\text{RF},\mathcal{S}_{N_t^{\text{RF}}}\|_2}\}\right). \quad (16)$$

For the FS, the optimization problem (5) can be simplified to (see Appendix A)

$$\begin{aligned} & \max_{\mathbf{F}_{\text{RF}}} \sum_{k=1}^K \|\mathbf{F}_{\text{opt}}^H[k] \bar{\mathbf{F}}_{\text{RF}}\|_F^2, \\ \text{s.t. } & \bar{\mathbf{F}}_{\text{RF}} = \text{blkdiag}\left(\frac{\mathbf{f}_{\text{RF},\mathcal{S}_1}}{\|\mathbf{f}_{\text{RF},\mathcal{S}_1}\|_2}, \dots, \frac{\mathbf{f}_{\text{RF},\mathcal{S}_{N_t^{\text{RF}}}}}{\|\mathbf{f}_{\text{RF},\mathcal{S}_{N_t^{\text{RF}}}\|_2}\}\right), \quad (17) \\ & \mathbf{f}_{\text{RF},\mathcal{S}_r} \in \mathcal{F}_{\text{RF},\mathcal{S}}, \text{ for } 1 \leq r \leq N_t^{\text{RF}}, \end{aligned}$$

where $\mathcal{F}_{\text{RF},\mathcal{S}}$ is a set of feasible RF precoder satisfying constant-modulus constraint, and the optimal fully-digital precoder $\mathbf{F}_{\text{opt}}[k]$ can be expressed as following block matrix form

$$\mathbf{F}_{\text{opt}}^H[k] = \left[\mathbf{F}_{\text{opt},\mathcal{S}_1}^H[k] \ \dots \ \mathbf{F}_{\text{opt},\mathcal{S}_{N_t^{\text{RF}}}}^H[k] \right], \quad (18)$$

and $\mathbf{F}_{\text{opt},\mathcal{S}_r}[k] \in \mathbb{C}^{N_t^{\text{sub}} \times N_t^{\text{RF}}}$ ($1 \leq k \leq K$). In solving (17), we use the following proposition.

Proposition 3. For FS, considering $\mathbf{F}_{\mathcal{S}_r} = [\mathbf{F}_{\text{opt},\mathcal{S}_r}[1] \ \dots \ \mathbf{F}_{\text{opt},\mathcal{S}_r}[K]]$, the RF precoder \mathbf{F}_{RF} solution to (17) is $\mathbf{F} = \text{blkdiag}(\mathbf{f}_{\text{RF},\mathcal{S}_1}, \dots, \mathbf{f}_{\text{RF},\mathcal{S}_{N_t^{\text{RF}}}})$, where $\mathbf{f}_{\text{RF},\mathcal{S}_r} = \alpha_r \mathbf{u}_{\mathcal{S}_r,1}$, for $r=1, \dots, N_t^{\text{RF}}$, $\alpha_r \in \mathbb{C}$ is a random complex number, and $\mathbf{u}_{\mathcal{S}_r,1}$ is the right singular vector corresponding with the largest singular value of the matrix $\mathbf{F}_{\mathcal{S}_r}$.

Proof. By substituting (16) and (18) into (17), the objective function of the optimization problem (17) can be further expressed as

$$\begin{aligned} & \sum_{k=1}^K \|\mathbf{F}_{\text{opt}}^H[k] \bar{\mathbf{F}}_{\text{RF}}\|_F^2 \\ &= \sum_{k=1}^K \left\| \begin{bmatrix} \mathbf{f}_{\text{RF},\mathcal{S}_1} \mathbf{F}_{\text{opt},\mathcal{S}_1}^H[k] & \dots & \mathbf{f}_{\text{RF},\mathcal{S}_{N_t^{\text{RF}}}} \mathbf{F}_{\text{opt},\mathcal{S}_{N_t^{\text{RF}}}}^H[k] \end{bmatrix} \right\|_F^2 \\ &= \sum_{r=1}^{N_t^{\text{RF}}} \frac{\sum_{k=1}^K \|\mathbf{f}_{\text{RF},\mathcal{S}_r} \mathbf{F}_{\text{opt},\mathcal{S}_r}^H[k]\|_2^2}{\|\mathbf{f}_{\text{RF},\mathcal{S}_r}\|_2^2} = \sum_{r=1}^{N_t^{\text{RF}}} \frac{\mathbf{f}_{\text{RF},\mathcal{S}_r} \mathbf{F}_{\mathcal{S}_r}^H \mathbf{F}_{\mathcal{S}_r} \mathbf{f}_{\text{RF},\mathcal{S}_r}^H}{\|\mathbf{f}_{\text{RF},\mathcal{S}_r}\|_2^2} \quad (19) \end{aligned}$$

Therefore, the solution to the optimization problem (17) is

$$\begin{aligned} & \max_{\mathbf{F}_{\text{RF}}} \sum_{k=1}^K \|\bar{\mathbf{F}}_{\text{RF}} \mathbf{F}_{\text{opt}}^H[k]\|_F^2 \\ &= \max_{\mathbf{F}_{\text{RF}}} \sum_{r=1}^{N_t^{\text{RF}}} \frac{\mathbf{f}_{\text{RF},\mathcal{S}_r} \mathbf{F}_{\mathcal{S}_r}^H \mathbf{F}_{\mathcal{S}_r} \mathbf{f}_{\text{RF},\mathcal{S}_r}^H}{\|\mathbf{f}_{\text{RF},\mathcal{S}_r}\|_2^2} = \sum_{r=1}^{N_t^{\text{RF}}} \lambda_1^2(\mathbf{F}_{\mathcal{S}_r}). \quad (20) \end{aligned}$$

The maximum value can only be obtained when $\mathbf{f}_{\text{RF},\mathcal{S}_r} = \alpha_r \mathbf{u}_{\mathcal{S}_r,1}$, where α_r is a complex value, and $\mathbf{u}_{\mathcal{S}_r,1}$ is the left singular vector of the largest singular value of the matrix $\mathbf{F}_{\mathcal{S}_r}$. \square

Finally, by taking the constant-modulus constraint into account, the final analog precoder matrix \mathbf{F}_{RF} can be obtained as $[\mathbf{f}_{\text{RF},\mathcal{S}_r}]_i = e^{j\angle([\mathbf{u}_{\mathcal{S}_r,1}]_i)}/\sqrt{N_t^{\text{sub}}}$ similar to (10). Given the RF precoder design for FS, the associated baseband precoder can be obtained according to (7).

At the receiver, we consider the subset of antenna indices associated with the r th RF chain as $\mathcal{T}_r = \{(r-1)N_r^{\text{sub}} +$

$1, \dots, rN_r^{\text{sub}}\}$, for $1 \leq r \leq N_r^{\text{RF}}$, where the cardinality of \mathcal{T}_r is $N_r^{\text{sub}} = N_r/N_r^{\text{RF}}$. Therefore, the analog combiner $\mathbf{W}_{\text{RF}} = \text{blkdiag}(\mathbf{w}_{\text{RF},\mathcal{T}_1}, \dots, \mathbf{w}_{\text{RF},\mathcal{T}_{N_r^{\text{RF}}}})$ and the baseband combiner $\mathbf{W}_{\text{BB}}[k] = [\mathbf{w}_{\text{BB},\mathcal{T}_1}[k] \ \dots \ \mathbf{w}_{\text{BB},\mathcal{T}_{N_r^{\text{RF}}}}[k]]$, where $\mathbf{w}_{\text{BB},\mathcal{T}_r}[k]$ is the baseband combiner vector associated with the r th receive subarray. Hence, we further obtain

$$\mathbf{W}_{\text{RF}} \mathbf{W}_{\text{BB}}[k] = \left[\mathbf{w}_{\text{RF},\mathcal{T}_1} \mathbf{w}_{\text{BB},\mathcal{T}_1}^H[k] \ \dots \ \mathbf{w}_{\text{RF},\mathcal{T}_{N_r^{\text{RF}}}} \mathbf{w}_{\text{BB},\mathcal{T}_{N_r^{\text{RF}}}}^H[k] \right]^T. \quad (21)$$

Moreover, we consider the effective channel

$$\mathbf{H}_{\text{eff}}[k] = \mathbf{H}[k] \mathbf{F}_{\text{RF}} \mathbf{F}_{\text{BB}}[k], \quad (22)$$

and the received signal (1) can be written as

$$\begin{aligned} & \begin{bmatrix} \mathbf{y}_{\mathcal{T}_1}[k] \\ \vdots \\ \mathbf{y}_{\mathcal{T}_{N_r^{\text{RF}}}}[k] \end{bmatrix} = \mathbf{y}[k] = \mathbf{H}_{\text{eff}}[k] \mathbf{x}[k] + \mathbf{n}[k] \\ &= \begin{bmatrix} \mathbf{H}_{\text{eff},\mathcal{T}_1}[k] \mathbf{x}[k] + \mathbf{n}_{\mathcal{T}_1}[k] \\ \vdots \\ \mathbf{H}_{\text{eff},\mathcal{T}_{N_r^{\text{RF}}}}[k] \mathbf{x}[k] + \mathbf{n}_{\mathcal{T}_{N_r^{\text{RF}}}}[k] \end{bmatrix}. \end{aligned} \quad (23)$$

By substituting (23) into (12), we have

$$\begin{aligned} & \sum_{k=1}^K \mathbb{E}[\|\mathbf{x}[k] - \mathbf{W}_{\text{BB}}^H[k] \mathbf{W}_{\text{RF}}^H \mathbf{y}[k]\|_2^2] = \sum_{k=1}^K (\text{Tr}(\mathbb{E}[\mathbf{x}[k] \mathbf{x}^H[k]])) \\ & - 2 \sum_{r=1}^{N_r^{\text{RF}}} \Re\{\text{Tr}(\mathbb{E}[\mathbf{x}[k] \mathbf{y}_{\mathcal{T}_r}^H[k]] \mathbf{w}_{\text{RF},\mathcal{T}_r} \mathbf{w}_{\text{BB},\mathcal{T}_r}^H[k])\} \\ & + \sum_{r=1}^{N_r^{\text{RF}}} \text{Tr}(\mathbf{w}_{\text{BB},\mathcal{T}_r}[k] \mathbf{w}_{\text{RF},\mathcal{T}_r}^H \mathbb{E}[\mathbf{y}_{\mathcal{T}_r}[k] \mathbf{y}_{\mathcal{T}_r}^H[k]] \mathbf{w}_{\text{RF},\mathcal{T}_r} \mathbf{w}_{\text{BB},\mathcal{T}_r}^H[k]), \end{aligned} \quad (24)$$

where $\mathbb{E}[\mathbf{y}_{\mathcal{T}_r}[k] \mathbf{y}_{\mathcal{T}_r}^H[k]] = \mathbf{H}_{\text{eff},\mathcal{T}_r}[k] \mathbf{H}_{\text{eff},\mathcal{T}_r}^H[k] + \sigma_n^2 \mathbf{I}_{N_r^{\text{sub}}}$. To design the $\{\mathbf{W}_{\text{BB}}[k]\}_{k=1}^K$ and \mathbf{W}_{RF} for minimizing (24), we first consider the optimal fully-digital combiner based on MMSE criterion, which can be expressed as $\mathbf{W}_{\text{opt}}^H[k] = [\mathbf{W}_{\text{opt},\mathcal{T}_1}^H[k] \ \dots \ \mathbf{W}_{\text{opt},\mathcal{T}_{N_r^{\text{RF}}}}^H[k]]$, for $1 \leq k \leq K$. To further simplify (24), we add a constant term irrelevant to the optimization object variables $\{\mathbf{W}_{\text{BB}}[k]\}_{k=1}^K$ and \mathbf{W}_{RF} in (24). Specifically, by adding $\sum_{k=1}^K \sum_{r=1}^{N_r^{\text{RF}}} \text{Tr}(\mathbf{W}_{\text{opt},\mathcal{T}_r}^H[k] \mathbb{E}[\mathbf{y}_{\mathcal{T}_r}[k] \mathbf{y}_{\mathcal{T}_r}^H[k]] \times \mathbf{W}_{\text{opt},\mathcal{T}_r}[k]) - \sum_{k=1}^K \text{Tr}(\mathbb{E}[\mathbf{x}[k] \mathbf{x}^H[k]])$ to (24), we have

$$\sum_{k=1}^K \sum_{r=1}^{N_r^{\text{RF}}} \|\mathbb{E}[\mathbf{y}_{\mathcal{T}_r}[k] \mathbf{y}_{\mathcal{T}_r}^H[k]]^{\frac{1}{2}} (\mathbf{W}_{\text{opt},\mathcal{T}_r}[k] - \mathbf{w}_{\text{RF},\mathcal{T}_r} \mathbf{w}_{\text{BB},\mathcal{T}_r}^H[k])\|_F^2. \quad (25)$$

The $\mathbf{w}_{\text{RF},\mathcal{T}_r}$ minimizing (25) is

$$\mathbf{w}_{\text{RF},\mathcal{T}_r} = \beta_r \mathbf{u}_{\mathcal{T}_r,1}, \quad (26)$$

where $\mathbf{u}_{\mathcal{T}_r,1}$ is the left singular vector associated with the largest singular value of the matrix $\mathbf{W}_{\mathcal{T}_r} = [\mathbb{E}[\mathbf{y}_{\mathcal{T}_r}[1] \mathbf{y}_{\mathcal{T}_r}^H[1]]^{\frac{1}{2}} \mathbf{W}_{\text{opt},\mathcal{T}_r}[1] \dots \mathbb{E}[\mathbf{y}_{\mathcal{T}_r}[K] \mathbf{y}_{\mathcal{T}_r}^H[K]]^{\frac{1}{2}} \cdot \mathbf{W}_{\text{opt},\mathcal{T}_r}[K]]$, and β_r is an arbitrary complex number. The specific proof is similar to that of Proposition 3. Given the RF combiner design for FS, the baseband combiner can be obtained by Algorithm 3.

B. AS Antenna Grouping for Precoder/Combiner

In previous subsection, we observed that the SE performance of FS depends heavily on $\{\mathbf{F}_{\mathcal{S}_r}\}_{r=1}^{N_t^{\text{RF}}}$ and $\{\mathbf{W}_{\mathcal{T}_r}\}_{r=1}^{N_t^{\text{RF}}}$. This observation motivates us to optimize the antenna grouping $\{\mathcal{S}_r\}_{r=1}^{N_t^{\text{RF}}}$ and $\{\mathcal{T}_r\}_{r=1}^{N_t^{\text{RF}}}$ to further improve the SE performance when AS is considered. Given the suitable antenna grouping, the rest hybrid precoder/combiner design for AS reduces to that for FS, which has been discussed in Subsection A.

At the transmitter, the optimization of transmit antenna grouping $\{\mathcal{S}_r\}_{r=1}^{N_t^{\text{RF}}}$ can be formulated as the following optimization problem

$$\begin{aligned} & \max_{\mathcal{S}_1, \dots, \mathcal{S}_{N_t^{\text{RF}}}} \sum_{r=1}^{N_t^{\text{RF}}} \lambda_1^2(\mathbf{F}_{\mathcal{S}_r}) \\ \text{s.t. } & \bigcup_{r=1}^{N_t^{\text{RF}}} \mathcal{S}_r = \{1, \dots, N_t\}, \mathcal{S}_i \cap \mathcal{S}_j = \emptyset \text{ for } i \neq j, \mathcal{S}_r \neq \emptyset \forall r. \end{aligned} \quad (27)$$

This optimization problem is a combinatorial optimization problem, which requires an exhaustive search to reach the optimal solution. The number of all possible combinations to obtain the optimal solution is $\frac{1}{(N_t^{\text{RF}})!} \sum_{n=0}^{N_t^{\text{RF}}} (-1)^{N_t^{\text{RF}}-n} \binom{N_t^{\text{RF}}}{n} n^{N_t}$ according to [29], which is clearly humongous. For example, when $N_t = 64$ and $N_t^{\text{RF}} = 4$, the number of all possible combinations can be up to 1.4178×10^{37} .

In this subsection, we focus on the design of a low-complexity antenna grouping algorithm to find the near-optimal solution to (27). Specifically, we first consider the approximation of $\lambda_1^2(\mathbf{F}_{\mathcal{S}_r})$ for the r th transmit subarray as below

$$\begin{aligned} \lambda_1^2(\mathbf{F}_{\mathcal{S}_r}) &= \lambda_1(\mathbf{R}_{\mathcal{S}_r}) \approx \frac{1}{\text{card}(\mathcal{S}_r)} \sum_{i=1}^{\text{card}(\mathcal{S}_r)} \sum_{j=1}^{\text{card}(\mathcal{S}_r)} |[\mathbf{R}_{\mathcal{S}_r}]_{i,j}| \\ &= \frac{1}{\text{card}(\mathcal{S}_r)} \sum_{i \in \mathcal{S}_r} \sum_{j \in \mathcal{S}_r} |[\mathbf{R}_F]_{i,j}|, \end{aligned} \quad (28)$$

where the first equation is due to the fact that the square of the singular value of the matrix $\mathbf{F}_{\mathcal{S}_r}$ is the eigenvalue of the matrix $\mathbf{R}_{\mathcal{S}_r} = \mathbf{F}_{\mathcal{S}_r} \mathbf{F}_{\mathcal{S}_r}^H$, and the second approximation is due to the tight lower bound and upper bound of $\lambda_1(\mathbf{R}_{\mathcal{S}_r})$ as proven in [22]. Based on (28), the objective function of the problem (27) becomes $\sum_{r=1}^{N_t^{\text{RF}}} 1/\text{card}(\mathcal{S}_r) \sum_{i \in \mathcal{S}_r} \sum_{j \in \mathcal{S}_r} |[\mathbf{R}_F]_{i,j}|$. This is a combinatorial optimization problem, and solving this requires exhaustive search with high-complexity.

To reduce the complexity while achieving good SE performance, we consider the antenna grouping from the viewpoint of clustering analysis in machine learning. Since the clustering metric here \mathbf{R}_F is more of a correlation-based rather than distance-based metric, we consider correlation based clustering method. To be specific, we propose a shared-AHC algorithm as listed in Algorithm 4, which is developed from the AHC algorithm to group the antennas into different subarrays associated with different RF chains. Traditional AHC algorithm is a clustering algorithm that builds a cluster hierarchy from

Algorithm 4 Shared Agglomerative Hierarchical Clustering (Shared-AHC) Algorithm for Antenna Grouping in AS.

Input: The correlation matrix $\mathbf{R}_F = \mathbf{F}\mathbf{F}^H$, number of antennas N_t , number of RF chains N_t^{RF} .
Output: Antenna grouping results $\mathcal{S}_1, \dots, \mathcal{S}_{N_t^{\text{RF}}}$.

```

1:  $N_{\text{sub}} = N_t, \mathcal{S}_i = \{i\}$  for  $i = 1, \dots, N_t$ 
2: while  $N_{\text{sub}} > N_t^{\text{RF}}$  do
3:    $\mathcal{S}_i^0 = \mathcal{S}_i$  for  $i = 1, \dots, N_{\text{sub}}$ ,  $n_{\text{sub}} = 1$ 
4:   for  $i = 1 : N_{\text{sub}}$  do
5:     if  $\exists r_0$  s.t.  $\mathcal{S}_i^0 \in \mathcal{S}_{r_0}$  then continue
6:     else if  $i = N_{\text{sub}}$  then  $\mathcal{S}_{n_{\text{sub}}} = \mathcal{S}_i^0$ 
7:     else
8:        $j = \arg \max_{l \in \{i+1, \dots, N_{\text{sub}}\}} g(\mathcal{S}_i, \mathcal{S}_l)$ 
9:        $i^0 = \arg \max_{l \in \{1, \dots, N_{\text{sub}}\} \setminus \{j\}} g(\mathcal{S}_j, \mathcal{S}_l)$ 
10:      if  $i = i^0$  then  $\mathcal{S}_{n_{\text{sub}}} = \mathcal{S}_i \cup \mathcal{S}_j$ 
11:      else  $\mathcal{S}_{n_{\text{sub}}} = \mathcal{S}_i$ 
12:      end if
13:    end if
14:     $n_{\text{sub}} = n_{\text{sub}} + 1$ 
15:  end for
16:   $N_{\text{sub}}^0 = n_{\text{sub}} - 1$ 
17:  if  $N_{\text{sub}}^0 < N_t^{\text{RF}}$  then  $\mathcal{S}_i = \mathcal{S}_i^0$  for  $i = 1, \dots, N_{\text{sub}}$ 
break
18:  else  $N_{\text{sub}} = N_{\text{sub}}^0$ 
19:  end if
20: end while
21: if  $N_{\text{sub}} > N_t^{\text{RF}}$  then sort  $\mathcal{S}_i$  according to the ascending order of cardinality
22:   for  $i = 1 : N_t^{\text{RF}} - N_{\text{sub}}$  do  $j = \arg \max_{l \in \{N_t^{\text{RF}} - N_{\text{sub}} + 1, \dots, N_{\text{sub}}\}} g(\mathcal{S}_i, \mathcal{S}_l), \mathcal{S}_i = \mathcal{S}_i \cup \mathcal{S}_j$ 
23:   end for
24:   Rearrange the subscript to guarantee that the order of subscripts are from 1 to  $N_t^{\text{RF}}$ 
25: end if

```

the bottom up. It starts by adding all data to multiple clusters, followed by iteratively pair-wise merging these clusters until only one cluster is left at the top of the hierarchy. The shared-AHC algorithm is different from the traditional AHC algorithm [25] in two distinguished aspects. First, the aim of clustering in our antenna grouping problem is to build N_t^{RF} clusters instead of only one cluster in conventional AHC algorithm. Second, the pair-wise merging criterion in the proposed algorithm is “shared”, while the conventional AHC algorithm only considers the target cluster. To further illustrate the “shared” mechanism, we introduce the metric of mutual correlation $g(\mathcal{S}_n, \mathcal{S}_m)$ between the cluster \mathcal{S}_n and \mathcal{S}_m

$$g(\mathcal{S}_n, \mathcal{S}_m) = \frac{1}{\text{card}(\mathcal{S}_n)\text{card}(\mathcal{S}_m)} \sum_{i \in \mathcal{S}_n} \sum_{j \in \mathcal{S}_m} |[\mathbf{R}_F]_{i,j}|. \quad (29)$$

In each clustering iteration, we first focus on a cluster \mathcal{S}_n , and find a cluster \mathcal{S}_m that maximizes $g(\mathcal{S}_n, \mathcal{S}_l)$ among all possible \mathcal{S}_l . If the cluster \mathcal{S}_n also maximizes $g(\mathcal{S}_m, \mathcal{S}_l)$ among

all possible \mathcal{S}_l , we merge \mathcal{S}_n and \mathcal{S}_m . Otherwise, the cluster \mathcal{S}_n and cluster \mathcal{S}_m are not merged and algorithm goes into the next iteration. Therefore, our proposed algorithm is featured as “shared”, since two clusters mutually share the maximum correlation in the sense of (29).

The proposed shared-AHC algorithm is listed in Algorithm 4. In step 1, the clusters are initialized. Steps 2-20 are the main body of the shared-AHC algorithm. Step 3 saves the clustering results in the last iteration and initializes the clustering process counter n_{sub} . Steps 5-6 consider the special situation that the target cluster is already merged into a former cluster (step 5) and the situation that the target cluster is $\mathcal{S}_{N_{\text{sub}}}$ and not merged into any of the former clusters (step 6). Steps 7-13 are the main shared-AHC clustering process. For the target cluster \mathcal{S}_i , \mathcal{S}_j is the cluster maximizing the correlation $g(\mathcal{S}_i, \mathcal{S}_l)$ within all the clusters that have not been searched for $i+1 \leq l \leq N_{\text{sub}}$ (step 8). For the chosen cluster \mathcal{S}_j , we need to make sure \mathcal{S}_j and \mathcal{S}_i have the maximum mutually correlation. Hence, we define cluster \mathcal{S}_{i^0} as the cluster maximizing the correlation $g(\mathcal{S}_i, \mathcal{S}_l)$ within all the clusters at current iteration (step 9). If $i = i^0$, cluster \mathcal{S}_i and cluster \mathcal{S}_j are merged (step 10). Otherwise, the cluster \mathcal{S}_j is not combined with cluster \mathcal{S}_i (step 11). After processing the target cluster \mathcal{S}_i , the cluster counter n_{sub} is increased by one and the next target cluster will be processed (step 14). After processing all the clusters in this loop, the stop criterion (steps 17-19) will be considered. If the resulting number of clusters $N_{\text{sub}} < N_t^{\text{RF}}$, the iteration process stops and the clustering result of the last iteration (step 17) will be considered. Otherwise, we continue the iteration (step 18). Steps 21-25 are the subsequent processing for the shared-AHC algorithm to make sure the result $N_{\text{sub}} = N_t^{\text{RF}}$. If $N_{\text{sub}} > N_t^{\text{RF}}$, the $(N_{\text{sub}} - N_t^{\text{RF}})$ clusters with $(N_{\text{sub}} - N_t^{\text{RF}})$ smallest cardinality are merged within the rest N_t^{RF} clusters (steps 21-23). Step 24 guarantees that the subscripts of clustering result match the notation of RF chains.

Note that, although the AS antenna grouping utilized the instantaneous channel information $\mathbf{H}[k]$, the AS antenna grouping does not have to change rapidly. To explain this, we give following lemma.

Lemma 2. *In large antenna scenario, i.e. $N_t \rightarrow \infty$, the matric of antenna grouping \mathbf{R}_F only determined by the steering vectors of N_s maximum amplitudes.*

Proof. Considering the large antenna regime, the transmit and receive steering vectors of channel $\mathbf{H}[k]$ are asymptotic orthogonal [8]. So the SVD of channel $\mathbf{H}[k]$ in (6) can be expressed as

$$\begin{aligned} \mathbf{U}[k] &= [\mathbf{A}_r \quad \mathbf{U}_r], \quad \Sigma[k] = \text{blkdiag}(|\mathbf{P}[k]|, \mathbf{0}), \\ \mathbf{V}[k] &= \text{blkdiag}(e^{j\angle\mathbf{P}[k]}, \mathbf{I}) [\mathbf{A}_t \quad \mathbf{V}_t], \end{aligned} \quad (30)$$

where $\mathbf{P}[k]$ is the frequency-domain channel matrix in which the diagonal elements are arranged by the descending order of the modulus, \mathbf{A}_r and \mathbf{A}_t are the corresponding matrices formed by the receive and transmit steering vectors, and \mathbf{U}_r and \mathbf{V}_t are random simi-unitary matrices. Note that the frequency-domain channel matrix $\mathbf{P}[k] = \sum_{d=0}^{D-1} \text{diag}(p_{1,1}[d], \dots, p_{N_{\text{cl}}, N_{\text{ray}}}[d]) e^{-j\frac{2\pi k}{K}d}$. Considering Dirac delta function as the pulse shaping filter, thus

$|\mathbf{P}[k]| = \sqrt{N_t N_r / (N_{\text{cl}} N_{\text{ray}})} \text{diag}(\alpha_{1,1}, \dots, \alpha_{N_{\text{cl}}, N_{\text{ray}}})$, which is irrelevant with k . Therefore, the steering vectors concerning with maximum N_s amplitudes $|\mathbf{P}[k]|_{i,i}$ ($i = 1, \dots, N_s$) remain unchange over different subcarriers. We denote the matrix of these steering vectors as $\mathbf{A}_{t,\text{max}}$. Thus, we have $\mathbf{F}_{\text{opt}}[1] = \dots = \mathbf{F}_{\text{opt}}[K] = \mathbf{A}_{t,\text{max}}$. Therefore, $\mathbf{R}_F = \mathbf{F}\mathbf{F}^H = \mathbf{K}\mathbf{A}_{t,\text{max}}\mathbf{A}_{t,\text{max}}^H$. \square

Actually, the channel matrix usually changes continuously according to time. In other words, the direction and amplitude of the main paths remain unchanged in a period of time. In fact, only the phase of channel gain changes rapidly, which is irrelevant to the AS grouping matric. Therefore, the AS antenna grouping can remain effective in enough amount of time and does not have to change when the channel changes.

At the receiver, we design the hybrid combiner antenna grouping for AS. To decouple $\mathbf{w}_{\text{RF}, \mathcal{T}_r}$ and $\{\mathbf{w}_{\text{BB}, \mathcal{T}_r}[k]\}_{k=1}^K$ in (25), we rewrite the problem (12) as

$$\begin{aligned} &\min_{\{\mathbf{w}_{\text{RF}, \mathcal{T}_r}\}_{r=1}^{N_r^{\text{RF}}}, \{\mathbf{w}_{\text{BB}, \mathcal{T}_r}[k]\}_{k=1, r=1}^{K, N_r^{\text{RF}}}} \sum_{k=1}^K \sum_{r=1}^{N_r^{\text{RF}}} \|\mathbb{E}[\mathbf{y}_{\mathcal{T}_r}[k]\mathbf{y}_{\mathcal{T}_r}^H[k]]\|^{\frac{1}{2}} \\ &\quad \cdot (\mathbf{W}_{\text{opt}, \mathcal{T}_r}[k] - \mathbf{w}_{\text{RF}, \mathcal{T}_r}\mathbf{w}_{\text{BB}, \mathcal{T}_r}^H[k])\|_F^2 \\ &\text{s.t. } \mathbf{w}_{\text{RF}, \mathcal{T}_r} \in \mathcal{W}_{\text{RF}, \mathcal{T}_r}, \end{aligned} \quad (31)$$

where $\mathcal{W}_{\text{RF}, \mathcal{T}_r}$ is a set of feasible RF combiner satisfying the constant-modulus constraint. Given the RF combiner $\mathbf{w}_{\text{RF}, \mathcal{T}_r}$ design, problem (31) is equivalent to the following problem

$$\begin{aligned} &\min_{\{\mathbf{w}_{\text{BB}, \mathcal{T}_r}[k]\}_{k=1}^K} \sum_{k=1}^K \|\mathbb{E}[\mathbf{y}_{\mathcal{T}_r}[k]\mathbf{y}_{\mathcal{T}_r}^H[k]]\|^{\frac{1}{2}} (\mathbf{W}_{\text{opt}, \mathcal{T}_r}[k] \\ &\quad - \mathbf{w}_{\text{RF}, \mathcal{T}_r}\mathbf{w}_{\text{BB}, \mathcal{T}_r}^H[k])\|_F^2, \end{aligned} \quad (32)$$

for $1 \leq r \leq N_r^{\text{RF}}$. Baseband combiner can be obtained by weighted LS as below

$$\begin{aligned} \mathbf{w}_{\text{BB}, \mathcal{T}_r}[k] &= (\mathbf{w}_{\text{RF}, \mathcal{T}_r}^H \mathbb{E}[\mathbf{y}_{\mathcal{T}_r}[k]\mathbf{y}_{\mathcal{T}_r}^H[k]] \mathbf{w}_{\text{RF}, \mathcal{T}_r})^{-1} \\ &\quad \cdot \mathbf{w}_{\text{RF}, \mathcal{T}_r}^H \mathbb{E}[\mathbf{y}_{\mathcal{T}_r}[k]\mathbf{y}_{\mathcal{T}_r}^H[k]] \mathbf{W}_{\text{opt}, \mathcal{T}_r}[k]. \end{aligned} \quad (33)$$

By substituting (33) into (25), we obtain

$$\begin{aligned} &\sum_{k=1}^K \sum_{r=1}^{N_r^{\text{RF}}} \text{Tr}(\mathbf{W}_{\text{opt}, \mathcal{T}_r}^H[k] \mathbb{E}[\mathbf{y}_{\mathcal{T}_r}[k]\mathbf{y}_{\mathcal{T}_r}^H[k]] \mathbf{W}_{\text{opt}, \mathcal{T}_r}[k] \\ &\quad - \mathbf{W}_{\text{opt}, \mathcal{T}_r}^H[k] \mathbb{E}[\mathbf{y}_{\mathcal{T}_r}[k]\mathbf{y}_{\mathcal{T}_r}^H[k]] \mathbf{w}_{\text{RF}, \mathcal{T}_r} \\ &\quad \cdot (\mathbf{w}_{\text{RF}, \mathcal{T}_r}^H \mathbb{E}[\mathbf{y}_{\mathcal{T}_r}[k]\mathbf{y}_{\mathcal{T}_r}^H[k]] \mathbf{w}_{\text{RF}, \mathcal{T}_r})^{-1} \\ &\quad \cdot \mathbf{w}_{\text{RF}, \mathcal{T}_r}^H \mathbb{E}[\mathbf{y}_{\mathcal{T}_r}[k]\mathbf{y}_{\mathcal{T}_r}^H[k]] \mathbf{W}_{\text{opt}, \mathcal{T}_r}[k]). \end{aligned} \quad (34)$$

Note that minimizing (34) is equivalent to maximizing the following function

$$\begin{aligned} &\sum_{k=1}^K \sum_{r=1}^{N_r^{\text{RF}}} \text{Tr}(\mathbf{W}_{\text{opt}, \mathcal{T}_r}^H[k] \mathbb{E}[\mathbf{y}_{\mathcal{T}_r}[k]\mathbf{y}_{\mathcal{T}_r}^H[k]] \mathbf{w}_{\text{RF}, \mathcal{T}_r} \\ &\quad \cdot (\mathbf{w}_{\text{RF}, \mathcal{T}_r}^H \mathbb{E}[\mathbf{y}_{\mathcal{T}_r}[k]\mathbf{y}_{\mathcal{T}_r}^H[k]] \mathbf{w}_{\text{RF}, \mathcal{T}_r})^{-1} \\ &\quad \cdot \mathbf{w}_{\text{RF}, \mathcal{T}_r}^H \mathbb{E}[\mathbf{y}_{\mathcal{T}_r}[k]\mathbf{y}_{\mathcal{T}_r}^H[k]] \mathbf{W}_{\text{opt}, \mathcal{T}_r}[k]). \end{aligned} \quad (35)$$

Furthermore, we assume

$$\mathbb{E}[\mathbf{y}_{\mathcal{T}_r}[1]\mathbf{y}_{\mathcal{T}_r}^H[1]] \approx \dots \approx \mathbb{E}[\mathbf{y}_{\mathcal{T}_r}[K]\mathbf{y}_{\mathcal{T}_r}^H[K]] \approx \mathbb{E}[\mathbf{y}_{\mathcal{T}_r}\mathbf{y}_{\mathcal{T}_r}^H], \quad (36)$$

for $1 \leq r \leq N_r^{\text{RF}}$. It should be pointed out that the approximation error in (36) can be ignored in large antennas regime as proven in Appendix D. Based on (36), the objective function (35) can be approximately expressed as

$$\begin{aligned}
& \sum_{k=1}^K \sum_{r=1}^{N_r^{\text{RF}}} \text{Tr}(\mathbf{W}_{\text{opt}, \mathcal{T}_r}^H[k] \mathbb{E}[\mathbf{y}_{\mathcal{T}_r} \mathbf{y}_{\mathcal{T}_r}^H] \mathbf{w}_{\text{RF}, \mathcal{T}_r} \\
& \cdot (\mathbf{w}_{\text{RF}, \mathcal{T}_r}^H \mathbb{E}[\mathbf{y}_{\mathcal{T}_r} \mathbf{y}_{\mathcal{T}_r}^H] \mathbf{w}_{\text{RF}, \mathcal{T}_r})^{-1} \mathbf{w}_{\text{RF}, \mathcal{T}_r}^H \mathbb{E}[\mathbf{y}_{\mathcal{T}_r} \mathbf{y}_{\mathcal{T}_r}^H] \mathbf{W}_{\text{opt}, \mathcal{T}_r}[k]) \\
& = \sum_{k=1}^K \sum_{r=1}^{N_r^{\text{RF}}} \frac{\|\mathbf{W}_{\text{opt}, \mathcal{T}_r}^H[k] \mathbb{E}[\mathbf{y}_{\mathcal{T}_r} \mathbf{y}_{\mathcal{T}_r}^H] \mathbf{w}_{\text{RF}, \mathcal{T}_r}\|_2^2}{\|\mathbb{E}[\mathbf{y}_{\mathcal{T}_r} \mathbf{y}_{\mathcal{T}_r}^H]^{\frac{1}{2}} \mathbf{w}_{\text{RF}, \mathcal{T}_r}\|_2^2} \\
& = \sum_{r=1}^{N_r^{\text{RF}}} \frac{\mathbf{w}_{\text{RF}, \mathcal{T}_r}^H \mathbb{E}[\mathbf{y}_{\mathcal{T}_r} \mathbf{y}_{\mathcal{T}_r}^H]^{\frac{1}{2}} \mathbf{W}_{\mathcal{T}_r} \mathbf{W}_{\mathcal{T}_r}^H \mathbb{E}[\mathbf{y}_{\mathcal{T}_r} \mathbf{y}_{\mathcal{T}_r}^H]^{\frac{1}{2}} \mathbf{w}_{\text{RF}, \mathcal{T}_r}}{\|\mathbb{E}[\mathbf{y}_{\mathcal{T}_r} \mathbf{y}_{\mathcal{T}_r}^H]^{\frac{1}{2}} \mathbf{w}_{\text{RF}, \mathcal{T}_r}\|_2^2}. \tag{37}
\end{aligned}$$

The maximum value of (37) is $\sum_{r=1}^{N_r^{\text{RF}}} \lambda_1^2(\mathbf{W}_{\mathcal{T}_r})$, when $\mathbf{w}_{\text{RF}, \mathcal{T}_r} = \beta_r \mathbf{u}_{\mathcal{T}_r, 1}$ according to (26). Therefore, the optimization of the receive antenna grouping $\{\mathcal{T}_r\}_{r=1}^{N_r^{\text{RF}}}$ can be expressed as the following optimization problem

$$\begin{aligned}
& \max_{\mathcal{T}_1, \dots, \mathcal{T}_{N_r^{\text{RF}}}} \sum_{r=1}^{N_r^{\text{RF}}} \lambda_1^2(\mathbf{W}_{\mathcal{T}_r}) \\
& \text{s.t. } \bigcup_{r=1}^{N_r^{\text{RF}}} \mathcal{T}_r = \{1, \dots, N_r\}, \mathcal{T}_i \cap \mathcal{T}_j = \emptyset \text{ for } i \neq j, \mathcal{T}_r \neq \emptyset \forall r. \tag{38}
\end{aligned}$$

Similar to (28), we further obtain

$$\begin{aligned}
\lambda_1^2(\mathbf{W}_{\mathcal{T}_r}) &= \lambda_1(\mathbf{R}_{\mathcal{T}_r}) \approx \frac{1}{\text{card}(\mathcal{T}_r)} \sum_{i=1}^{\text{card}(\mathcal{T}_r)} \sum_{j=1}^{\text{card}(\mathcal{T}_r)} |[\mathbf{R}_{\mathcal{T}_r}]_{i,j}| \\
&= \frac{1}{\text{card}(\mathcal{T}_r)} \sum_{i \in \mathcal{T}_r} \sum_{j \in \mathcal{T}_r} |[\mathbf{R}_W]_{i,j}|,
\end{aligned} \tag{39}$$

where $\mathbf{R}_{\mathcal{T}_r} = \mathbf{W}_{\mathcal{T}_r} \mathbf{W}_{\mathcal{T}_r}^H$ and $\mathbf{R}_W = \mathbf{W} \mathbf{W}^H$. The antenna grouping $\{\mathcal{T}_r\}_{r=1}^{N_r^{\text{RF}}}$ at the receiver can be obtained by using the proposed shared-AHC algorithm in Algorithm 4, where the corresponding inputs are weighted matrix \mathbf{R}_W , the number of receive antennas N_r , and the number of RF chains at the receiver N_r^{RF} .

V. PERFORMANCE EVALUATION

In this section, we will investigate the SE performance for the hybrid precoder design at the transmitter, the SE, BER and EE performance for the hybrid precoder/combiner design, and the performance the proposed shared-AHC based AS antenna grouping algorithm in both computational complexity and slow time-varying feature. For the channel model, we adopt Dirac delta function as the pulse shaping filter and a cyclic prefix with the length of $D = 64$. The number of subcarriers is $K = 512$. The carrier frequency is $f_c = 30$ GHz, and the transmission bandwidth is $B = 500$ MHz. We consider that the path delay is uniformly distributed in $[0, DT_s]$ ($T_s = 1/B$ is the symbol period). The number of the clusters is $N_{\text{cl}} = 8$, and the angle spread of each cluster is 7.5° regardless of azimuth or elevation for both AoD and AoA. Within each cluster, there are $N_{\text{ray}} = 10$ rays. As for the antennas, we consider

(a)	(b)	(c)	(d)

Fig. 1. Four types of FS: (a) Vertical type; (b) Horizontal type; (c) Squared type; (d) Interlaced type.

both the transmitter and receiver adopt 8×8 UPA, and the distance between each adjacent antennas is half wavelength. Moreover, we consider the number of RF chains at transmitter and receiver are $N_t^{\text{RF}} = N_r^{\text{RF}} = 4$ and the data stream is $N_s = 3$ unless otherwise stated. Additionally, we consider 4 types of classical FS patterns as shown in Fig. 1, where antenna elements with the same color share the same RF chain.

The following baselines will be compared as benchmarks: **Optimal fully-digital** scheme considers the fully-digital MIMO system, where the SVD-based precoder/combiner is adopted as the performance upper bound. **Simultaneous OMP (SOMP)** scheme is an extended version of the narrow-band OMP-based spatially sparse precoding in [15]. In broadband, SOMP-based hybrid precoding scheme can simultaneously design the RF precoder/combiner for all subcarriers. **Discrete Fourier transform (DFT) codebook** scheme designs the RF precoder/combiner from the DFT codebook instead of steering vectors codebook in SOMP scheme [35]. **Covariance eigenvalue decomposition (EVD)** scheme estimates the covariance matrix of the channels using the mean of auto-correlation matrices at each subcarrier [22]. The RF precoder is designed based on the EVD of the covariance matrix of the channels.

A. Numerical Simulation on SE Performance

In this subsection, we simulate the SE performance at transmitter and the whole transmitter-receiver system.

In Fig. 2, we compare the SE performance of the proposed hybrid precoding scheme at the transmitter with four baseline schemes mentioned previously, where both FCA and PCS (including FS and AS) are investigated in Fig. 2 (a) and (b), respectively. Both the infinite quantized phase shifters ($Q = \infty$) and limited quantized phase shifters ($Q = 3$ and $Q = 1$) are investigated. It should be pointed out that in Fig. 2, we only compare the performance of transmit hybrid precoder, where the fully-digital receiver is assumed. For FCA, it can be observed from Fig. 2 (a) that our proposed PCA-based hybrid precoding scheme outperforms conventional DFT codebook-based hybrid precoding scheme and SOMP-based hybrid precoding scheme. This is because that mmWave MIMO channels associated with different subcarriers share the same row space due to the common scatterers. Meanwhile, our proposed algorithm can exploit the principal components of the common row space to establish the hybrid precoder. The SOMP-based and DFT codebook-based hybrid precoding schemes perform poorly since their analog codebooks are limited to the steering vector forms. Additionally, it can also be observed from Fig. 2 that the influence of quantization over

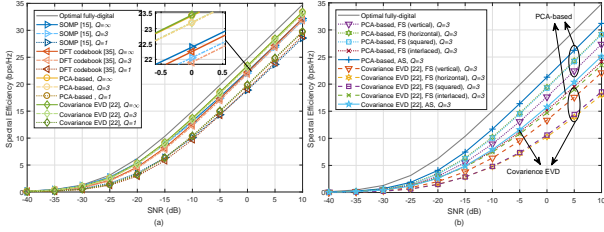


Fig. 2. SE performance comparison of different hybrid precoder schemes, where both transmitter and receiver employ 8×8 UPA, $N_t^{\text{RF}} = 4$, $K = 512$, and the fully-digital array is considered at the receiver: (a) FCA with $Q = \infty$, $Q = 3$ and $Q = 1$; (b) PCS with typical quantization $Q = 3$.

3 bits in phase shifters can be negligible and the worst 1-bit quantization does not influence much. As for the PCS, we consider a typical 3-bit quantization for phase shifter in Fig. 2 (b), which shows that our scheme outperforms conventional covariance EVD-based hybrid precoder design scheme with different FS patterns and AS. The antenna grouping scheme in [22] is based on the greedy search, which may lead to the imbalance antenna grouping, since the local optimal solution may be acquired. By contrast, the shared-AHC-based antenna grouping algorithm introduces the mutually correlation metric (29), which can effectively avoid this issue. Therefore, the proposed shared-AHC-based antenna grouping algorithm outperforms its counterpart in [22].

In Fig. 3, we evaluate SE performance of the proposed PCA-based hybrid precoding scheme, SOMP-based hybrid precoding scheme, and DFT codebook-based hybrid precoding scheme, where both hybrid precoder and combiner are jointly investigated, and $Q = \infty$, $Q = 3$ and $Q = 1$ are considered, respectively. For FS, both the transmitter and receiver share the same antenna grouping pattern. As shown in Fig. 3 (a), the proposed PCA-based hybrid precoding scheme outperforms the SOMP-based hybrid precoding scheme and DFT codebook-based hybrid precoding scheme when FCA is considered. The DFT codebook-based hybrid precoding scheme works poorly due to the quantization loss of the DFT codebook with limited size. Additionally, quantization over 3 bits can be negligible and influence of quantization in worst 1-bit case is limited. As shown in Fig. 3 (b) for PCS in typical quantization $Q = 3$ case, the performance of FS varies with the different FS patterns, and AS consistently outperforms the FS with four typical patterns. This is because different channel matrix can have different spatial features depending on the different spatial scatterers. An FS pattern suitable for one kind of channels may not be suitable for another kind of channels. Therefore, to achieve improved SE performance, the antenna array pattern should be adaptive to the specific channels. The proposed shared-AHC algorithm in AS can dynamically adjust the antenna pattern according to the spatial feature of practical channels, and thus the improved SE performance can be achieved.

B. Numerical Simulation on BER Performance

In this subsection, we simulate the BER performance of the system. In Fig. 4, we evaluate the BER performance of the

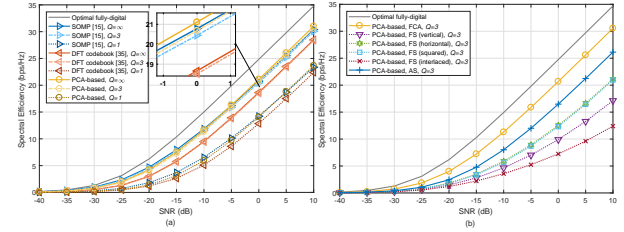


Fig. 3. SE performance comparison of different hybrid precoding schemes, where both transmitter and receiver employ 8×8 UPA, $N_t^{\text{RF}} = N_r^{\text{RF}} = 4$, and $K = 512$: (a) FCA with $Q = \infty$, $Q = 3$ and $Q = 1$; (b) PCS with typical quantization $Q = 3$.

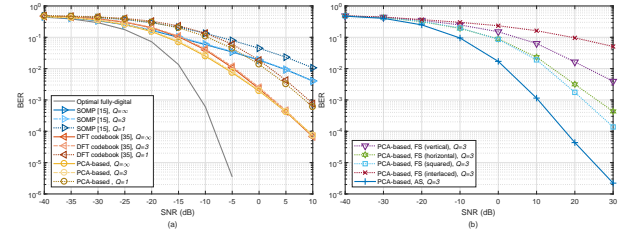


Fig. 4. BER performance comparison of different hybrid precoding schemes, where both transmitter and receiver employ 8×8 UPA, $N_t^{\text{RF}} = N_r^{\text{RF}} = 4$, and $K = 128$: (a) FCA with $Q = \infty$, $Q = 3$ and $Q = 1$; (b) PCS with typical quantization $Q = 3$.

proposed PCA-based hybrid precoding scheme, SOMP-based hybrid precoding scheme, and DFT codebook-based hybrid precoding scheme, where both hybrid precoder and combiner are jointly investigated, 16 QAM is adopted for transmission, and $Q = \infty$, $Q = 3$ and $Q = 1$ are considered, respectively. As shown in Fig. 4 (a), the proposed PCA-based hybrid precoding scheme outperforms the conventional SOMP-based and DFT codebook-based hybrid precoding schemes in BER performance for FCA. Additionally, quantization over 3 bits can be negligible and influence of quantization in worst 1 bit case is limited. As shown in Fig. 4 (b) for PCS in typical quantization $Q = 3$ case, the performance of FS varies with the different patterns, and AS consistently outperforms the FS in BER performance. This is because AS implements the shared-AHC algorithm for antenna grouping, thus the antenna pattern can dynamically adapt to the spatial feature of different channels.

C. EE Performance Analysis and Numerical Simulation

In this subsection, we analyze the EE performance of the system and do numerical simulation on EE performance. Specifically, we define the EE metric as $\eta = RB/P$, where B is the transmission bandwidth, R is the SE in (3), and P is the total power consumption of the system. From Fig. 1, we can observe that FCA and PCS have different power consumption due to the different numbers of phase shifters. Take transmitter for example, FCA requires $N_t N_t^{\text{RF}} = 256$ phase shifters for connecting each RF chain to all antennas, while the PCS only requires $N_t = 64$ phase shifters. Furthermore, different antenna architectures should also be taken into account due to the different total power. Specifically, we consider the hybrid MIMO systems using passive antennas and active antennas

as shown in Fig. 2 (a) and (b), respectively. Both of them consist of analog-digital/digital-analog convertors (AD/DA), low noise amplifiers (LNA), power amplifiers (PA), local oscillators (LO), duplexers or switches (DPX/S), and mixers etc. It is worth mentioning that DPX/S is used to transmit and receive signals sharing the same antenna hardware. When working in transmitting mode, the DPX/S ensures the transmit signal delivered from PA to antennas. When working in receiving mode, the DPX/S ensures the receive signal delivered from antennas to LNA. So the power consumption of DPX/S can be negligible since the switching duration between the transmitting mode and receiving mode can be neglected. As for the active and passive antenna architecture, the main difference lies in the position of the PAs/LNAs. In passive antennas, the number of PAs/LNAs is the same as that of the RF chains. While for active antennas, the number of PAs/LNAs is the same as that of antennas. This difference can lead to different power consumption because the PAs/LNAs consume large power. Thus we will analyze the power consumption for two different antenna architectures, respectively. Given the passive antenna architecture in Fig. 2 (a), the power consumption for FCA and PCS are respectively $P_{FCA}^p = N_t^{\text{RF}}(P_{\text{DA}} + P_{\text{mix}} + P_{\text{LO}} + P_{\text{PA}}) + N_t N_t^{\text{RF}} P_{\text{PS}} + N_r^{\text{RF}}(P_{\text{AD}} + P_{\text{mix}} + P_{\text{LO}} + P_{\text{LNA}}) + N_r N_r^{\text{RF}} P_{\text{PS}} + 2P_{\text{syn}}$ and $P_{\text{PCS}}^p = N_t^{\text{RF}}(P_{\text{DA}} + P_{\text{mix}} + P_{\text{LO}} + P_{\text{PA}}) + N_t P_{\text{PS}} + N_r^{\text{RF}}(P_{\text{AD}} + P_{\text{mix}} + P_{\text{LO}} + P_{\text{LNA}}) + N_r P_{\text{PS}} + 2P_{\text{syn}}$. By contrast, the power consumption for FCA and PCS with active antenna architecture as shown in Fig. 2 (b) are $P_{\text{FCA}}^a = N_t^{\text{RF}}(P_{\text{DA}} + P_{\text{mix}} + P_{\text{LO}}) + N_t N_t^{\text{RF}} P_{\text{PS}} + N_t P_{\text{PA}} + 2P_{\text{syn}} + N_r^{\text{RF}}(P_{\text{AD}} + P_{\text{mix}} + P_{\text{LO}}) + N_r N_r^{\text{RF}} P_{\text{PS}} + N_r P_{\text{LNA}}$ and $P_{\text{PCS}}^a = N_t^{\text{RF}}(P_{\text{DA}} + P_{\text{mix}} + P_{\text{LO}}) + N_t P_{\text{PS}} + N_t P_{\text{PA}} + 2P_{\text{syn}} + N_r^{\text{RF}}(P_{\text{AD}} + P_{\text{mix}} + P_{\text{LO}}) + N_r P_{\text{PS}} + N_r P_{\text{LNA}}$. Moreover, according to the antenna architecture for fully-digital (FD) precoder/combiner as shown in Fig. 2 (c), the power consumption is $P_{\text{FD}} = N_t(P_{\text{PA}} + P_{\text{DA}} + P_{\text{mix}} + P_{\text{LO}}) + 2P_{\text{syn}} + N_r(P_{\text{LNA}} + P_{\text{AD}} + P_{\text{mix}} + P_{\text{LO}})$. Additionally, the power values of electronic components constituting three antenna architectures are $P_{\text{PS}} = 15 \text{ mW}$ for 3-bit phase shifter [31], $P_{\text{AD}} = P_{\text{DA}} = 200 \text{ mW}$ for AD/DA [31], $P_{\text{mix}} = 39 \text{ mW}$ for mixer [32], $P_{\text{PA}} = 138 \text{ mW}$ for PA [33], $P_{\text{LNA}} = 39 \text{ mW}$ for LNA [33], $P_{\text{LO}} = 5 \text{ mW}$ for LO [31], and $P_{\text{syn}} = 50 \text{ mW}$ for synchronizer [34].

In Fig. 6, we compare the EE performance of the proposed PCA-based hybrid precoding scheme, SOMP-based hybrid precoding scheme, and DFT codebook-based hybrid precoding scheme in typical quantization $Q = 3$ case with FCA and PCS, where both passive and active antenna architectures are investigated. Note that the power values of key electronic components can refer to Section VI. In Fig. 6 (a), for passive antenna architecture, the EE performance of PCS by using the proposed PCA-based hybrid precoding scheme outperforms that of FCA by using the proposed and baseline schemes. The reason is that PCS adopts a much smaller number of phase shifters than FCA, though SE performance of PCS still suffer from a performance gap compared with FCA. Moreover, AS outperforms the other FS patterns in SE, and it consumes the same power with the other FS patterns. Therefore, AS outperforms other four types of FS patterns. Note that the optimal fully-digital scheme has the worst EE performance,

since the numbers of power-consuming PAs, LNAs, ADs/DAs, mixers are proportional to that of antennas. In Fig. 6 (b), the advantage of EE performance for different FS patterns by using the proposed hybrid precoding scheme over the FCA with several typical hybrid precoding schemes and fully-digital array with the optimal precoding scheme is not considerable. This is because active antenna architecture requires the power-hungry PAs/LNAs for each antenna. Meanwhile, the advantage of the reduced power consumption benefiting from FS structure is greatly weakened by its disadvantage in SE performance when compared with FCA. Finally, the EE performance of AS with the proposed hybrid precoding scheme still has obvious advantage over the other schemes. This observation reveals the appealing advantage of AS in practical situation when both the power consumption and SE should be well balanced.

D. Performance Analysis and Numerical Simulation for AS Grouping Algorithm

In this subsection, we compare the computational complexity of the proposed shared-AHC algorithm and the greedy algorithm in [22] for antenna grouping. Additionally, we investigate the influence of unchanged AS pattern under changing channel condition. The computational complexity of key steps in the shared-AHC algorithm and greedy algorithm is provided in Table I. Note that it is difficult to analyze the overall complexity of the shared-AHC algorithm and greedy algorithm directly due to the following reasons. First, both the computational complexity of shared-AHC algorithm and the greedy algorithm depends on the channel condition. Second, both two algorithms have the selection statements of “if” and “else”, and for different selections, the complexity can be different. Third, the total number of iterations for the shared-AHC algorithm is adaptive, and the complexity within each iteration depends on the condition of the former iteration. Considering these, we compare the computational complexity of the two algorithm according to their practical runtime. Fig. 7 (a) indicates the computational complexity of the proposed shared-AHC algorithm comparing with the greedy algorithm. The simulation is performed based on the software of MATLAB R2016a, and the computer configuration is Intel Core i7-7700 CPU and 16 GB RAM. The channel parameters are the same with previous simulations. We assume the numbers of transmit and receive antennas are $N_t = N_r \in \{4^2, 5^2, 6^2, \dots, 12^2\}$. Fig. 7 (a) shows the mean and standard deviation of the runtime of the proposed shared-AHC algorithm and the greedy algorithm in [22] for antenna grouping. We can observe from Fig. 7 (a) that the order of the mean runtime of the proposed shared-AHC algorithm is similar to that of the greedy algorithm, and the standard deviation of the proposed shared-AHC algorithm is larger than that of the greedy algorithm.

Since the direction of multipath changes slowly while the channel gain changes rapidly, we generate different channels and consider different time slots of one channel realization. In each time slot, the direction of multipath remains unchanged while only the phase of channel gain changes. For each realization of channels, we respectively investigate the SE performance under unchanged AS over all slots and changing

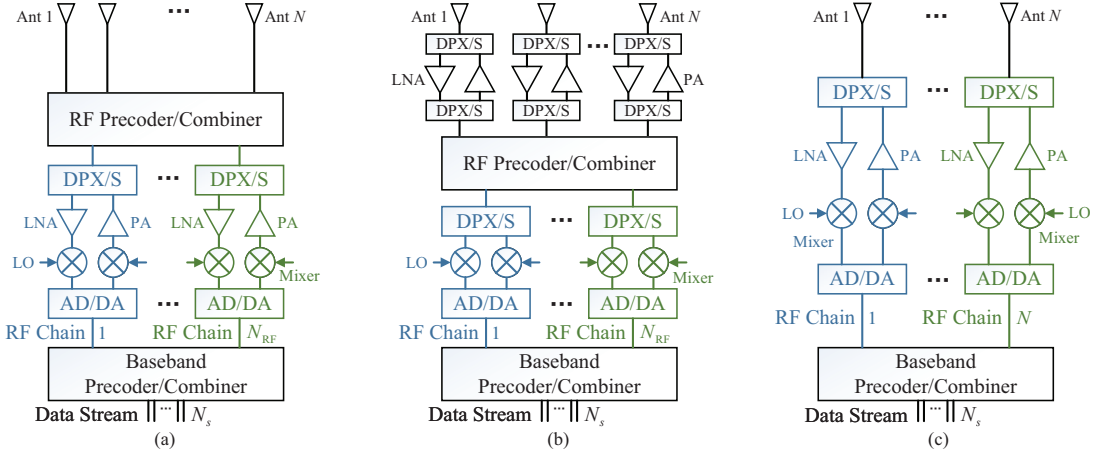


Fig. 5. Different antenna architectures: (a) Hybrid MIMO with passive antennas; (b) Hybrid MIMO with active antennas; (c) Fully-digital MIMO array [30].

TABLE I
COMPUTATIONAL COMPLEXITY

Shared-AHC Algorithm		Greedy Algorithm in [22]	
Operation	Complexity	Operation	Complexity
Step 2	$\min \log_2(N_t - N_t^{\text{RF}})$	Step 2	unclear
Step 4	N_{sub}	Step 3	$\frac{1}{2}N_t(N_t - 1)$
Step 8	$\text{card}(\mathcal{S}_i)(\sum_{l=i+1}^{N_{\text{sub}}} \text{card}(\mathcal{S}_l))$	Step 8	$\sum_{r=1}^{N_t^{\text{RF}}} ((\text{card}(\mathcal{S}_r) + 2)^2 + \text{card}(\mathcal{S}_r)^2)$
Step 9	$\text{card}(\mathcal{S}_j)(\sum_{l \in \{1, \dots, N_{\text{sub}}\} \setminus \{j\}} \text{card}(\mathcal{S}_l))$	Step 11	$\text{card}(\mathcal{S}_m)^2 + \text{card}(\mathcal{S}_n)^2$
Step 21	$\frac{N_{\text{sub}}}{N_{\text{sub}} - N_t^{\text{RF}}}$	Step 12	$(\text{card}(\mathcal{S}_m) + 1)^2 + (\text{card}(\mathcal{S}_n) - 1)^2$
Step 22	$\text{card}(\mathcal{S}_i)(\sum_{l=N_t^{\text{RF}} - N_{\text{sub}} + 1}^{N_{\text{sub}}} \text{card}(\mathcal{S}_l))$	Step 13	$(\text{card}(\mathcal{S}_m) - 1)^2 + (\text{card}(\mathcal{S}_n) + 1)^2$

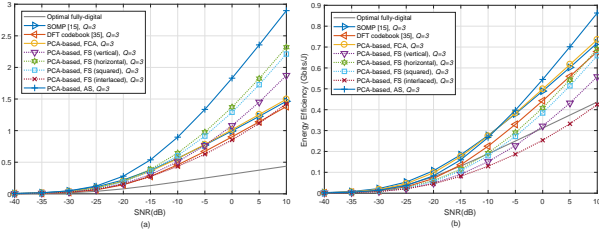


Fig. 6. EE performance comparison of different hybrid precoding schemes on different antenna architectures with typical phase shifter quantization $Q = 3$, where both the transmitter and receiver employ 8×8 UPA, $N_t^{\text{RF}} = N_r^{\text{RF}} = 4$, and $K = 512$: (a) Passive antenna; (b) Active antenna.

AS in each slot. We consider the receiver using fully-digital combiner and 2×2 UPA. Fig. 7 (b) shows the SE comparison between unchanged and changed AS when $\text{SNR}=0, 10$ and -10 dB. We can observe that there is no obvious SE performance gap between unchanged and changed AS. Therefore, the AS does not have to change rapidly with the channel.

VI. CONCLUSIONS

In this paper, we proposed a hybrid precoding scheme based on PCA for broadband mmWave MIMO systems. We first designed a low-dimensional frequency flat precoder/combiner from the optimal frequency-selective precoder/combiner based

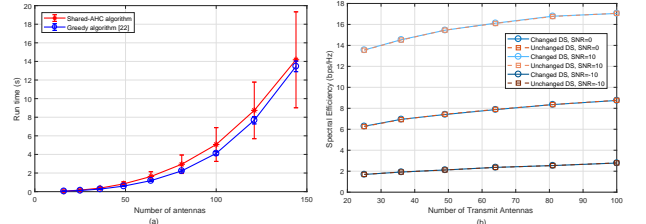


Fig. 7. Numerical Simulation for AS Grouping Algorithm: (a) Computational complexity comparison of the proposed shared-AHC algorithm and the conventional greedy algorithm; (b) SE performance comparison of the unchanged AS and changed AS.

on PCA for FCA. Moreover, we extended the proposed PCA-based hybrid precoder/combiner design to the PCS. We developed PCA-based precoding scheme under FS. We then proposed the shared-AHC algorithm inspired by cluster analysis in the field of machine learning for antenna grouping to further improve the SE performance. Finally, we evaluated the SE and BER performance of the proposed PCA-based precoding scheme, analyzed the EE performance, and investigated the computational complexity and slow time-varying feature of the shared-AHC based AS antenna grouping algorithm.

APPENDIX A PROOF OF LEMMA 1

To start with, we make the following system approximation.

Approximation 1. We assume that the hybrid precoder $\mathbf{F}_{\text{RF}}\mathbf{F}_{\text{BB}}[k]$ can be sufficiently “close” to the optimal fully-digital precoder $\mathbf{F}_{\text{opt}}[k] = \mathbf{F}_{\text{RF}}\mathbf{F}_{\text{BB}}[k]$, for $1 \leq k \leq K$, under the given system model and parameters ($N_t, N_r, N_t^{\text{RF}}, N_r^{\text{RF}}, N_s, N_{\text{cl}}, N_{\text{ray}}, \dots$). Define $\Sigma[k] = \text{blkdiag}(\Sigma_1[k], \Sigma_2[k])$, where $\Sigma_1[k] = [\Sigma[k]]_{1:N_s, 1:N_s}$, and $\mathbf{V}[k] = [\mathbf{F}_{\text{opt}}[k] \ \mathbf{V}_2[k]]$ in (6), for $1 \leq k \leq K$, this “closeness” is defined based on the following two equivalent approximations:

- (1) The eigenvalues of the matrix $\mathbf{I}_{N_s} - \mathbf{F}_{\text{opt}}^H[k]\mathbf{F}_{\text{RF}}\mathbf{F}_{\text{BB}}[k]\mathbf{F}_{\text{BB}}^H[k]\mathbf{F}_{\text{RF}}^H\mathbf{F}_{\text{opt}}[k]$ are small. In this case, it can be equivalently stated as $\mathbf{F}_{\text{opt}}^H[k]\mathbf{F}_{\text{RF}}\mathbf{F}_{\text{BB}}[k] \approx \mathbf{I}_{N_s}$.
- (2) The singular values of the matrix $\mathbf{V}_2^H[k]\mathbf{F}_{\text{RF}}\mathbf{F}_{\text{BB}}[k]$ are small, i.e. $\mathbf{V}_2^H[k]\mathbf{F}_{\text{RF}}\mathbf{F}_{\text{BB}}[k] \approx \mathbf{0}$.

Following the similar steps of the equations (12) in [15], we first define (40) Based on the definition in (40), the objective function of problem (4) can be approximate as

$$\begin{aligned}
& \sum_{k=1}^K \log_2(\det(\mathbf{I}_{N_r} + \frac{1}{\sigma_n^2} \mathbf{H}[k]\mathbf{F}_{\text{RF}}\mathbf{F}_{\text{BB}}[k]\mathbf{F}_{\text{BB}}^H[k]\mathbf{F}_{\text{RF}}^H\mathbf{H}^H[k])) \\
&= \sum_{k=1}^K \log_2(\det(\mathbf{I}_{N_r} + \frac{1}{\sigma_n^2} \Sigma^2[k]\mathbf{V}^H[k]\mathbf{F}_{\text{RF}}\mathbf{F}_{\text{BB}}[k]\mathbf{F}_{\text{BB}}^H[k]\mathbf{F}_{\text{RF}}^H\mathbf{V}[k])) \\
&= \sum_{k=1}^K \log_2(\det(\mathbf{I}_{N_r} + \frac{1}{\sigma_n^2} \begin{bmatrix} \Sigma_1^2[k] & \mathbf{0} \\ \mathbf{0} & \Sigma_2^2[k] \end{bmatrix} \begin{bmatrix} \mathbf{M}_{11}[k] & \mathbf{M}_{12}[k] \\ \mathbf{M}_{21}[k] & \mathbf{M}_{22}[k] \end{bmatrix})) \\
&\stackrel{(a)}{=} \sum_{k=1}^K (\log_2(\det(\mathbf{I}_{N_s} + \frac{1}{\sigma_n^2} \Sigma_1^2[k]\mathbf{M}_{11}[k])) \\
&\quad + \log_2(\det(\mathbf{I} + \frac{1}{\sigma_n^2} \Sigma_2^2[k]\mathbf{M}_{22}[k] \\
&\quad - \frac{1}{\sigma_n^2} \Sigma_2^2[k]\mathbf{M}_{21}[k](\mathbf{I}_{N_s} + \frac{1}{\sigma_n^2} \Sigma_1^2[k]\mathbf{M}_{11}[k])^{-1}\Sigma_1^2[k]\mathbf{M}_{12}[k]))) \\
&\stackrel{(b)}{\approx} \sum_{k=1}^K \log_2(\det(\mathbf{I}_{N_s} \\
&\quad + \frac{1}{\sigma_n^2} \Sigma_1^2[k]\mathbf{F}_{\text{opt}}^H[k]\mathbf{F}_{\text{RF}}\mathbf{F}_{\text{BB}}[k]\mathbf{F}_{\text{BB}}^H[k]\mathbf{F}_{\text{RF}}^H\mathbf{F}_{\text{opt}}[k])), \tag{41}
\end{aligned}$$

where the equation and approximation are based on

- (a) is based on the Schur complement identity for matrix determinants.
- (b) is based on Approximation 1 (2), which implies that $\mathbf{M}_{21}[k]$, $\mathbf{M}_{12}[k]$, and $\mathbf{M}_{22}[k]$ are approximately 0. The equation can be obtained when $\Sigma_2[k] = \mathbf{0}$, a.k.a. the rank of channel matrix $\mathbf{H}[k]$ is N_s . Equation can be obtained when Approximation 1 obtained.

Inspired by equation (13)-(14) in [15], the function (41) can be further approximate as (42) where the approximations in (42) are based on

- (c) is based on $\mathbf{I} + \mathbf{B}\mathbf{A} = (\mathbf{I} + \mathbf{B})(\mathbf{I} - (\mathbf{I} + \mathbf{B})^{-1}\mathbf{B}(\mathbf{I} - \mathbf{A}))$ with definition $\mathbf{B} = \Sigma_1^2/\sigma_n^2$ and $\mathbf{A} = \mathbf{F}_{\text{opt}}^H[k]\mathbf{F}_{\text{RF}}\mathbf{F}_{\text{BB}}[k]\mathbf{F}_{\text{BB}}^H[k]\mathbf{F}_{\text{RF}}^H\mathbf{F}_{\text{opt}}[k]$.
- (d) is based on Approximation 1 (2), which implies the eigenvalues of matrix $(\mathbf{I}_{N_s} + \frac{1}{\sigma_n^2} \Sigma_1^2[k])^{-1}\Sigma_1^2[k]/\sigma_n^2$ are

small. So, $\log_2(\det(\mathbf{I}_{N_s} - \mathbf{X})) \approx \log_2(1 - \text{Tr}(\mathbf{X})) \approx -\text{Tr}(\mathbf{X})$. Equation can be obtained when Approximation 1 obtained.

- (e) is based on SNR approximation $(\mathbf{I} + \Sigma_1^2/\sigma_n^2)\Sigma_1^2/\sigma_n^2 \approx \mathbf{I}_{N_s}$. Equation can be obtained at high SNR.

Therefore, the optimization problem (4) can be approximate as (9).

APPENDIX B PROOF OF PROPOSITION 1

Defining the SVD of $\mathbf{F}_{\text{RF}} = \mathbf{U}_{\text{RF}}\Sigma_{\text{RF}}\mathbf{V}_{\text{RF}}^H$, the equation (7) can be written as $\mathbf{F}_{\text{BB}}[k] = \mathbf{V}_{\text{RF}}\Sigma_{\text{RF}}^{-1}\mathbf{V}_{\text{RF}}^H\mathbf{F}_{\text{BB}}[k]$. Combining $\mathbf{F}_{\text{BB}}[k]$ with the optimization problem in (9), the objective function can be written as

$$\sum_{k=1}^K \|\mathbf{F}_{\text{opt}}^H[k]\mathbf{U}_{\text{RF}}\mathbf{V}_{\text{RF}}\mathbf{F}_{\text{BB}}[k]\|_F^2. \tag{43}$$

According to previous work [28], unitary constraints offer a close performance to the total power constraint while providing a relatively simple form of solution. To simplify the problem, we consider the condition under unitary power constraints instead. Therefore, water-filling power allocation coefficients can be ignored. Specifically, the equivalent baseband precoder is $\tilde{\mathbf{F}}_{\text{BB}}[k] = [\tilde{\mathbf{V}}[k]]_{:,1:N_s}$. Hence, $\mathbf{F}_{\text{BB}}[k]$ is a unitary or semi-unitary matrix, which depends on the relationship between N_s and N_t^{RF} . Therefore, in the following part, we discuss the two conditions separately.

When $N_s = N_t^{\text{RF}}$, $\tilde{\mathbf{F}}_{\text{BB}}[k]$ is a unitary matrix. Therefore, (43) can be simplified as

$$\begin{aligned}
& \sum_{k=1}^K \|\mathbf{F}_{\text{opt}}^H[k]\mathbf{U}_{\text{RF}}\mathbf{V}_{\text{RF}}\tilde{\mathbf{F}}_{\text{BB}}[k]\|_F^2 \\
&= \text{Tr}\left(\sum_{k=1}^K \mathbf{U}_{\text{RF}}^H\mathbf{F}_{\text{opt}}[k]\mathbf{F}_{\text{opt}}^H[k]\mathbf{U}_{\text{RF}}\right) \\
&= \text{Tr}\left(\left[\mathbf{U}_{\text{RF}}^H\mathbf{F}_{\text{opt}}[1] \ \cdots \ \mathbf{U}_{\text{RF}}^H\mathbf{F}_{\text{opt}}[K]\right] \begin{bmatrix} \mathbf{F}_{\text{opt}}^H[1]\mathbf{U}_{\text{RF}} \\ \vdots \\ \mathbf{F}_{\text{opt}}^H[K]\mathbf{U}_{\text{RF}} \end{bmatrix}\right) \\
&= \text{Tr}(\mathbf{U}_{\text{RF}}^H\mathbf{F}\mathbf{F}^H\mathbf{U}_{\text{RF}}) = \text{Tr}(\mathbf{U}_{\text{RF}}^H\mathbf{U}_F\Sigma_F^2\mathbf{U}_F^H\mathbf{U}_{\text{RF}}). \tag{44}
\end{aligned}$$

Since both \mathbf{U}_{RF} and \mathbf{U}_F are unitary matrix, (44) reaches the maximum only when $\mathbf{U}_{\text{RF}} = \mathbf{U}_F$. Moreover, the rank of \mathbf{F}_{RF} is N_t^{RF} . Hence, $\mathbf{U}_{\text{RF}} = [\mathbf{U}_F]_{:,1:N_t^{\text{RF}}}\mathbf{U}_R$. Hence, the optimal RF precoder can be expressed as $\mathbf{F}_{\text{RF}} = [\mathbf{U}_F]_{:,1:N_t^{\text{RF}}}\mathbf{U}_R\Sigma_{\text{RF}}\mathbf{V}_{\text{RF}}^H = \mathbf{U}_F\mathbf{R}_t$, where $\mathbf{R}_t = \mathbf{U}_R\Sigma_{\text{RF}}\mathbf{V}_{\text{RF}}^H \in \mathbb{C}^{N_t^{\text{RF}} \times N_t^{\text{RF}}}$ is an arbitrary full rank matrix.

When $N_s < N_t^{\text{RF}}$, $\tilde{\mathbf{F}}_{\text{BB}}[k]$ is a semi-unitary matrix. Defining the SVD $\tilde{\mathbf{F}}_{\text{BB}}[k] = \mathbf{U}_{\text{BB}}[k]\begin{bmatrix} \mathbf{I}_{N_s} & \mathbf{0} \end{bmatrix}^T \times \mathbf{V}_{\text{BB}}^H[k]$, the objective function (43) can be simplified as

$$\begin{aligned}
& \sum_{k=1}^K \text{Tr}(\mathbf{F}_{\text{opt}}^H[k]\mathbf{U}_{\text{RF}}\mathbf{V}_{\text{RF}}\mathbf{U}_{\text{BB}}[k]\text{blkdiag}(\mathbf{I}_{N_s}, \mathbf{0}) \\
& \quad \times \mathbf{U}_{\text{BB}}^H[k]\mathbf{V}_{\text{RF}}^H\mathbf{U}_{\text{RF}}^H\mathbf{F}_{\text{opt}}[k]). \tag{45}
\end{aligned}$$

It is obvious that the solution satisfying (44) also satisfies (45). Therefore, following the similar derivation of (44), the conclusion of $\mathbf{F}_{\text{RF}} = \mathbf{U}_F\mathbf{R}_t$ is easy to be reached.

$$\begin{aligned} & \mathbf{V}^H[k] \mathbf{F}_{\text{RF}} \mathbf{F}_{\text{BB}}[k] \mathbf{F}_{\text{BB}}^H[k] \mathbf{F}_{\text{RF}}^H \mathbf{V}[k] \\ &= \begin{bmatrix} \mathbf{F}_{\text{opt}}^H[k] \mathbf{F}_{\text{RF}} \mathbf{F}_{\text{BB}}[k] \mathbf{F}_{\text{BB}}^H[k] \mathbf{F}_{\text{RF}}^H \mathbf{F}_{\text{opt}}[k] & \mathbf{F}_{\text{opt}}^H[k] \mathbf{F}_{\text{RF}} \mathbf{F}_{\text{BB}}[k] \mathbf{F}_{\text{BB}}^H[k] \mathbf{F}_{\text{RF}}^H \mathbf{V}_2[k] \\ \mathbf{V}_2^H[k] \mathbf{F}_{\text{RF}} \mathbf{F}_{\text{BB}}[k] \mathbf{F}_{\text{BB}}^H[k] \mathbf{F}_{\text{RF}}^H \mathbf{F}_{\text{opt}}[k] & \mathbf{V}_2^H[k] \mathbf{F}_{\text{RF}} \mathbf{F}_{\text{BB}}[k] \mathbf{F}_{\text{BB}}^H[k] \mathbf{F}_{\text{RF}}^H \mathbf{V}_2[k] \end{bmatrix} = \begin{bmatrix} \mathbf{M}_{11}[k] & \mathbf{M}_{12}[k] \\ \mathbf{M}_{21}[k] & \mathbf{M}_{22}[k] \end{bmatrix} \end{aligned} \quad (40)$$

$$\begin{aligned} & \sum_{k=1}^K \log_2 (\det(\mathbf{I}_{N_s} + \frac{1}{\sigma_n^2} \boldsymbol{\Sigma}_1^2[k] \mathbf{F}_{\text{opt}}^H[k] \mathbf{F}_{\text{RF}} \mathbf{F}_{\text{BB}}[k] \mathbf{F}_{\text{BB}}^H[k] \mathbf{F}_{\text{RF}}^H \mathbf{F}_{\text{opt}}[k])) \\ & \stackrel{(c)}{=} \sum_{k=1}^K (\log_2 (\det(\mathbf{I}_{N_s} + \frac{1}{\sigma_n^2} \boldsymbol{\Sigma}_1^2[k]))) \\ & \quad + \log_2 (\det(\mathbf{I}_{N_s} - (\mathbf{I}_{N_s} + \frac{1}{\sigma_n^2} \boldsymbol{\Sigma}_1^2[k]))^{-1} \frac{1}{\sigma_n^2} \boldsymbol{\Sigma}_1^2[k] (\mathbf{I}_{N_s} - \mathbf{F}_{\text{opt}}^H[k] \mathbf{F}_{\text{RF}} \mathbf{F}_{\text{BB}}[k] \mathbf{F}_{\text{BB}}^H[k] \mathbf{F}_{\text{RF}}^H \mathbf{F}_{\text{opt}}[k]))) \\ & \stackrel{(d)}{\approx} \sum_{k=1}^K (\log_2 (\det(\mathbf{I}_{N_s} + \frac{1}{\sigma_n^2} \boldsymbol{\Sigma}_1^2[k]))) \\ & \quad - \text{Tr}((\mathbf{I}_{N_s} + \frac{1}{\sigma_n^2} \boldsymbol{\Sigma}_1^2[k])^{-1} \frac{1}{\sigma_n^2} \boldsymbol{\Sigma}_1^2[k] (\mathbf{I}_{N_s} - \mathbf{F}_{\text{opt}}^H[k] \mathbf{F}_{\text{RF}} \mathbf{F}_{\text{BB}}[k] \mathbf{F}_{\text{BB}}^H[k] \mathbf{F}_{\text{RF}}^H \mathbf{F}_{\text{opt}}[k]))) \\ & \stackrel{(e)}{\approx} \sum_{k=1}^K (\log_2 (\det(\mathbf{I}_{N_s} + \frac{1}{\sigma_n^2} \boldsymbol{\Sigma}_1^2[k])) - \text{Tr}((\mathbf{I}_{N_s} - \mathbf{F}_{\text{opt}}^H[k] \mathbf{F}_{\text{RF}} \mathbf{F}_{\text{BB}}[k] \mathbf{F}_{\text{BB}}^H[k] \mathbf{F}_{\text{RF}}^H \mathbf{F}_{\text{opt}}[k]))) \\ &= \sum_{k=1}^K (\log_2 (\det(\mathbf{I}_{N_s} + \frac{1}{\sigma_n^2} \boldsymbol{\Sigma}_1^2[k])) - (N_s - \|\mathbf{F}_{\text{opt}}^H[k] \mathbf{F}_{\text{RF}} \mathbf{F}_{\text{BB}}[k]\|_F^2)). \end{aligned} \quad (42)$$

APPENDIX C PROOF OF PROPOSITION 2

Substituting the weighted LS estimation for baseband combiner in (15) into the objective function of (14), we obtain

$$\begin{aligned} & \sum_{k=1}^K \|\mathbb{E}[\mathbf{y}[k]\mathbf{y}^H[k]]^{\frac{1}{2}}(\mathbf{W}_{\text{opt}}[k] - \mathbf{W}_{\text{RF}}\mathbf{W}_{\text{BB}}[k])\|_F^2 \\ &= \sum_{k=1}^K \|\mathbb{E}[\mathbf{y}[k]\mathbf{y}^H[k]]^{\frac{1}{2}}\mathbf{W}_{\text{opt}}[k] \\ & \quad - \mathbb{E}[\mathbf{y}[k]\mathbf{y}^H[k]]^{\frac{1}{2}}\mathbf{W}_{\text{RF}}(\mathbf{W}_{\text{RF}}^H\mathbb{E}[\mathbf{y}[k]\mathbf{y}^H[k]]\mathbf{W}_{\text{RF}})^{-1} \\ & \quad \cdot \mathbf{W}_{\text{RF}}^H\mathbb{E}[\mathbf{y}[k]\mathbf{y}^H[k]]\mathbf{W}_{\text{opt}}[k]\|_F^2. \end{aligned} \quad (46)$$

Defining $\mathbf{A}[k] = \mathbb{E}[\mathbf{y}[k]\mathbf{y}^H[k]]^{\frac{1}{2}}\mathbf{W}_{\text{opt}}[k]$ and $\mathbf{B}[k] = \mathbb{E}[\mathbf{y}[k]\mathbf{y}^H[k]]^{\frac{1}{2}}\mathbf{W}_{\text{RF}}$, we further obtain

$$\begin{aligned} & \sum_{k=1}^K \|\mathbf{A}[k] - \mathbf{B}[k](\mathbf{B}^H[k]\mathbf{B}[k])^{-1}\mathbf{B}^H[k]\mathbf{A}[k]\|_F^2 \\ &= \sum_{k=1}^K \text{Tr}(\mathbf{A}^H[k]\mathbf{A}[k]) \\ & \quad - \sum_{k=1}^K \text{Tr}(\mathbf{A}^H[k]\mathbf{B}[k](\mathbf{B}^H[k]\mathbf{B}[k])^{-1}\mathbf{B}^H[k]\mathbf{A}[k]). \end{aligned} \quad (47)$$

Hence, the minimization problem can be formulated as the following maximization problem

$$\begin{aligned} & \max_{\mathbf{W}_{\text{RF}}, \mathbf{W}_{\text{BB}}[k]} \sum_{k=1}^K \text{Tr}(\mathbf{A}^H[k]\mathbf{B}[k](\mathbf{B}^H[k]\mathbf{B}[k])^{-1}\mathbf{B}^H[k]\mathbf{A}[k]) \\ & \text{s.t. } \mathbf{B}[k] = \mathbb{E}[\mathbf{y}[k]\mathbf{y}^H[k]]^{\frac{1}{2}}\mathbf{W}_{\text{RF}}, \mathbf{W}_{\text{RF}} \in \mathcal{W}_{\text{RF}}. \end{aligned} \quad (48)$$

Assuming the SVD of $\mathbf{B}[k] = \mathbf{U}_B[k]\boldsymbol{\Sigma}_B[k]\mathbf{V}_B^H[k]$, the objective function of the problem (48) can be written as $\sum_{k=1}^K \text{Tr}(\mathbf{A}^H[k]\mathbf{B}[k](\mathbf{B}^H[k]\mathbf{B}[k])^{-1}\mathbf{B}^H[k]\mathbf{A}[k]) = \sum_{k=1}^K \|\mathbf{U}_B^H[k]\mathbf{A}[k]\|_F^2$. Since $\mathbf{B}[k] = \mathbb{E}[\mathbf{y}[k]\mathbf{y}^H[k]]^{\frac{1}{2}}\mathbf{W}_{\text{RF}}$, we can find a matrix $\mathbf{R}_B[k] \in \mathbb{C}^{N_r^{\text{RF}} \times N_r^{\text{RF}}}$ satisfying $\mathbf{U}_B[k] = \mathbf{R}_B[k]\mathbf{U}_W$. Hence, the objective function of the optimization

problem (48) can be expressed as

$$\sum_{k=1}^K \|\mathbf{U}_B^H[k]\mathbf{A}[k]\|_F^2 = \sum_{k=1}^K \|\mathbf{U}_W^H \mathbf{R}_B^H[k]\mathbf{A}[k]\|_F^2. \quad (49)$$

Note that function (49) is similar to the objective function of maximization problem (9), thus $\mathbf{W}_{\text{RF}} = [\mathbf{U}_D]_{:,1:N_r^{\text{RF}}} \mathbf{R}_d$, where $\mathbf{R}_d \in \mathbb{C}^{N_r^{\text{RF}} \times N_r^{\text{RF}}}$ is a full-rank matrix and \mathbf{U}_D is the left singular matrix of $\mathbf{D} = [\mathbf{R}_B^H[1]\mathbf{A}[1] \cdots \mathbf{R}_B^H[K]\mathbf{A}[K]] = \text{blkdiag}(\mathbf{R}_B^H[1], \dots, \mathbf{R}_B^H[K])\mathbf{W}$. Assuming matrix $\mathbf{U}_R \in \mathbb{C}^{N_r^{\text{RF}} \times N_r^{\text{RF}}}$ satisfying $[\mathbf{U}_D]_{:,1:N_r^{\text{RF}}} = [\mathbf{U}_W]_{:,1:N_r^{\text{RF}}} \mathbf{U}_R$, the solution to problem (48) is $\mathbf{W}_{\text{RF}} = [\mathbf{U}_D]_{:,1:N_r^{\text{RF}}} \mathbf{R}_d = [\mathbf{U}_W]_{:,1:N_r^{\text{RF}}} \mathbf{U}_R \mathbf{R}_d = [\mathbf{U}_W]_{:,1:N_r^{\text{RF}}} \mathbf{R}_r$, where $\mathbf{R}_r = \mathbf{U}_R \mathbf{R}_d$ is an arbitrary full rank matrix.

APPENDIX D PROOF OF (36)

By substituting (6) and (7) into (22), we obtain $\mathbf{H}_{\text{eff}}[k] = \mathbf{H}[k]\mathbf{F}_{\text{RF}}\mathbf{F}_{\text{BB}}[k] = \mathbf{U}[k]\tilde{\mathbf{U}}[k]\tilde{\boldsymbol{\Sigma}}[k]\tilde{\mathbf{V}}^H[k]$ $\times [\tilde{\mathbf{V}}[k]]_{:,1:N_s} \mathbf{A}[k]$. Defining $[\tilde{\mathbf{V}}[k]]_{:,1:N_s} = \tilde{\mathbf{V}}_{N_s}[k]$ and $\tilde{\mathbf{V}}[k] = [\tilde{\mathbf{V}}_{N_s}[k] \quad \tilde{\mathbf{V}}_0[k]]$, $\mathbf{H}_{\text{eff}}[k]$ can be written as

$$\begin{aligned} \mathbf{H}_{\text{eff}}[k] &= \mathbf{U}[k]\tilde{\mathbf{U}}[k]\tilde{\boldsymbol{\Sigma}}[k] \begin{bmatrix} \tilde{\mathbf{V}}_{N_s}^H[k] \\ \tilde{\mathbf{V}}_0^H[k] \end{bmatrix} \tilde{\mathbf{V}}_{N_s}[k]\mathbf{A}[k] \\ &= [\mathbf{U}[k]\tilde{\mathbf{U}}[k]\tilde{\boldsymbol{\Sigma}}[k]]_{:,1:N_s} \mathbf{A}[k]. \end{aligned} \quad (50)$$

Combine (8) with (50), it arrives

$$\begin{aligned} \mathbf{H}_{\text{eff}}[k] &= [\mathbf{U}[k]\tilde{\mathbf{U}}[k]\tilde{\boldsymbol{\Sigma}}[k]]_{:,1:N_s} \mathbf{A}[k] \\ &= [\mathbf{U}[k]\tilde{\mathbf{U}}[k]]_{:,1:N_s} (\mu[\tilde{\boldsymbol{\Sigma}}[k]]_{1:N_s,1:N_s} - N_s \mathbf{I}_{N_s}). \end{aligned} \quad (51)$$

In large antenna, $\tilde{\mathbf{U}}[k] = \mathbf{I}$ and $\tilde{\boldsymbol{\Sigma}}[k] = \boldsymbol{\Sigma}[k]$. The effective channel can be further written as

$$\begin{aligned} \mathbf{H}_{\text{eff}}[k] &= [\mathbf{U}[k]]_{:,1:N_s} (\mu[\boldsymbol{\Sigma}[k]]_{1:N_s,1:N_s} - N_s \mathbf{I}_{N_s}) \\ &= [\mathbf{A}_r[k]]_{:,1:N_s} (\mu[\mathbf{P}[k]]_{1:N_s,1:N_s} - N_s \mathbf{I}_{N_s}). \end{aligned} \quad (52)$$

Considering (23), the effective channel matrix $\mathbf{H}_{\text{eff},\mathcal{T}_r}[k] = [\mathbf{A}_r]_{\mathcal{T}_r,1:N_s}(\mu[\|\mathbf{P}[k]\|]_{1:N_s,1:N_s} - N_s \mathbf{I}_{N_s})$. Therefore, the covariance matrix of $\mathbf{y}_{\mathcal{T}_r}[k]$ can be expressed as

$$\begin{aligned} \mathbb{E}[\mathbf{y}_{\mathcal{T}_r}[k]\mathbf{y}_{\mathcal{T}_r}^H[k]] &= \mathbf{H}_{\text{eff},\mathcal{T}_r}[k]\mathbf{H}_{\text{eff},\mathcal{T}_r}^H[k] + \sigma_n^2 \mathbf{I}_{N_s^{\text{sub}}} \\ &= [\mathbf{A}_r]_{\mathcal{T}_r,1:N_s}(\mu[\|\mathbf{P}[k]\|]_{1:N_s,1:N_s} - N_s \mathbf{I}_{N_s})^2 ([\mathbf{A}_r]_{\mathcal{T}_r,1:N_s})^H + \sigma_n^2 \mathbf{I}_{N_s^{\text{sub}}}. \end{aligned} \quad (53)$$

Note that $[\mathbf{P}[k]]$ is irrelevant with k . Therefore, $\mathbb{E}[\mathbf{y}_{\mathcal{T}_r}[k]\mathbf{y}_{\mathcal{T}_r}^H[k]]$ is irrelevant with k when the very large number of antennas is considered. In other words, (36) is valid in the regime of very large number of antennas, and this approximation usually holds for mmWave MIMO with large number of antennas.

REFERENCES

- [1] Yiwei Sun, Zhen Gao, Hua Wang, and Di Wu, "Machine learning based hybrid precoding for mmWave MIMO-OFDM with dynamic subarray," in *Proc. IEEE Global Commun. Conf. Workshop (GC Wkshps)*, Dec. 2018, pp. 1-6.
- [2] Yiwei Sun, Zhen Gao, Hua Wang, and Di Wu, "Wideband hybrid precoding for next-generation backhaul/fronthaul based on mmWave FD-MIMO," in *Proc. IEEE Global Commun. Conf. Workshop (GC Wkshps)*, Dec. 2018, pp. 1-6.
- [3] George C. Alexandropoulos, "Position aided beam alignment for millimeter wave backhaul systems with large phased arrays," in *Proc. IEEE International Workshop on Computational Advances in Multi-Sensor Adaptive Processing (CAMSAP)*, Dec. 2017, pp. 1-5.
- [4] Zhenyu Xiao, Lipeng Zhu, Jinho Choi, Pengfei Xia, and Xiang-Gen Xia, "Joint power allocation and beamforming for non-orthogonal multiple access (NOMA) in 5G millimeter wave communications," *IEEE Trans. Wireless Commun.*, vol. 17, no. 5, pp. 2961-2974, May 2018.
- [5] Yuhan Sun and Chenhao Qi, "Weighted sum-rate maximization for analog beamforming and combining in millimeter wave massive MIMO communications," *IEEE Commun. Lett.*, vol. 21, no. 8, pp. 1883-1886, Oct. 2017.
- [6] Evangelos Vlachos, George C. Alexandropoulos, and John Thompson, "Massive MIMO Channel Estimation for Millimeter Wave Systems via Matrix Completion," *IEEE Signal Process. Lett.*, vol. 25, no. 11, pp. 1675-1679, Nov. 2018.
- [7] Xincong Lin, Sheng Wu, Chunxiao Jiang, Linling Kuang, Jian Yan, and Lajos Hanzo, "Estimation of broadband multiuser millimeter wave massive MIMO-OFDM channels by exploiting their sparse structure," *IEEE Trans. Wireless Commun.*, vol. 17, no. 6, pp. 3959-3973, Jun. 2018.
- [8] Jiening Mao, Zhen Gao, Yongpeng Wu, and Mohamed-Slim Alouini, "Over-sampling codebook-based hybrid minimum sum-mean-square-error precoding for millimeter-wave 3D-MIMO," *IEEE Wireless Commun. Lett.*, vol. PP, no. PP, pp. 1-1, May 2018.
- [9] Yongming Huang, Jianjun Zhang, and Ming Xiao, "Constant envelope hybrid precoding for directional millimeter-wave communications," *IEEE J. Sel. Areas Commun.*, vol. PP, no. PP, pp. 1-1, Apr. 2018.
- [10] Shiwen He, Jiaheng Wang, Yongming Huang, Bjrn Ottersten, and Wei Hong, "Codebook-based hybrid precoding for millimeter wave multiuser systems," *IEEE Trans. Signal Process.*, vol. 65, no. 20, pp. 5289-5304, Oct. 2017.
- [11] An Liu, Vincent K. N. Lau, and Min-Jian Zhao, "Stochastic successive convex optimization for two-timescale hybrid precoding in massive MIMO," *IEEE J. Sel. Topics Signal Process.*, vol. 12, no. 3, pp. 432-444, June 2018.
- [12] George C. Alexandropoulos and Symeon Chouvardas, "Low Complexity Channel Estimation for Millimeter Wave Systems with Hybrid A/D Antenna Processing," in *Proc. IEEE Global Comm. Workshops (GC Wkshps)*, Dec. 2016, pp. 1-6.
- [13] Chongwen Huang, Lei Liu, Chau Yuen, and Sumei Sun, "A LSE and Sparse Message Passing-Based Channel Estimation for mmWave MIMO Systems," in *Proc. IEEE Global Comm. Workshops (GC Wkshps)*, Dec. 2016, pp. 1-6.
- [14] X. Zhu, Z. Wang, L. Dai, and Q. Wang, "Adaptive Hybrid Precoding for Multiuser Massive MIMO," *IEEE Communications Letters*, vol. 20, no. 4, pp. 776-779, Apr. 2016.
- [15] Omar El Ayach, Sridhar Rajagopal, Shadi Abu-Surra, Zhouyue Pi, and Robert W. Heath, "Spatially sparse precoding in millimeter wave MIMO systems," *IEEE Trans. Wireless Commun.*, vol. 13, no. 3, pp. 1499-1513, Mar. 2014.
- [16] Chiang-Hen Chen, Cheng-Rung Tsai, Yu-Hsin Liu, Wei-Lun Hung, and An-Yeu Wu, "Compressive sensing (CS) assisted low-complexity beamspace hybrid precoding for millimeter-wave MIMO Systems," *IEEE Trans. Signal Process.*, vol. 65, no. 6, pp. 1412-1424, Mar. 2017.
- [17] Omar El Ayach, Robert W. Heath, Sridhar Rajagopal, and Zhouyue Pi, "Multimode precoding in millimeter wave MIMO transmitters with multiple antenna sub-arrays," in *Proc. IEEE Global Commun. Conf. (GLOBECOM)*, Dec. 2013, pp. 3476-3480.
- [18] Weiheng Ni and Xiaodai Dong, "Hybrid block diagonalization for massive multiuser MIMO systems," *IEEE Trans. Commun.*, vol. 64, no. 1, pp. 201-211, Jan. 2016.
- [19] Foad Sohrabi and Wei Yu, "Hybrid digital and analog beamforming design for large-scale antenna arrays," *IEEE J. Sel. Topics Signal Process.*, vol. 10, no. 3, pp. 501-513, Apr. 2016.
- [20] Chanhong Kim, Taeyoung Kim, and Ji-Yun Seol, "Multi-beam transmission diversity with hybrid beamforming for MIMO-OFDM systems," in *Proc. IEEE Globecom Workshops (GC Wkshps)*, Dec. 2013, pp. 61-65.
- [21] Ahmed Alkhateeb and Robert W. Heath, "Frequency selective hybrid precoding for limited feedback millimeter wave systems," *IEEE Trans. Commun.*, vol. 64, no. 5, pp. 1801-1818, May 2016.
- [22] Sungwoo Park, Ahmed Alkhateeb, and Robert W. Heath, "Dynamic subarrays for hybrid precoding in wideband mmWave MIMO system," *IEEE Trans. Wireless Commun.*, vol. 16, no. 5, pp. 2907-2920, May 2017.
- [23] Kiran Venugopal, Nuria Gonzlez-Prelcic, and Robert W. Heath, "Optimality of frequency flat precoding in frequency selective millimeter wave channels," *IEEE Wireless Commun. Lett.*, vol. 6, no. 3, pp. 330-333, Jun. 2017.
- [24] Joseph Costantine, Youssef Tawk, Silvio E. Barbin, and Christos G. Christodoulou, "Reconfigurable antennas: Design and applications," *Proc. IEEE*, vol. 103, no. 3, pp. 424-437, Mar. 2015.
- [25] Shihbing Zhou, Zhenyuan Xu, and Fei Liu, "Method for determining the optimal number of clusters based on agglomerative hierarchical clustering," *IEEE Trans. Neural Netw. Learn. Syst.*, vol. 28, no. 12, pp. 3007-3017, Dec. 2017.
- [26] C. M. Bishop, *Pattern Recognition and Machine Learning*. New York, NY, USA: Springer, 2006.
- [27] Chongwen Huang, George C. Alexandropoulos, Alessio Zappone, Mérourane Debbah, and Chau Yuen, "Energy efficient multi-user MISO communication using low resolution large intelligent surfaces," in *Proc. IEEE Global Commun. Conf. (GLOBECOM)*, Dec. 2018, pp. 1-6.
- [28] David J. Love, Robert W. Heath, Vincent K. N. Lau, David Gesbert, Bhaskar D. Rao, and Matthew Andrews, "An overview of limited feedback in wireless communication systems," *IEEE J. Sel. Areas Commun.*, vol. 26, no. 8, pp. 1341-1365, Oct. 2008.
- [29] R. Graham *et al.*, *Concrete Mathematics*. Reading, MA, USA: Addison-Wesley, 1988.
- [30] Wei Hong, Zhi Hao Jiang, Chao Yu, Jianyi Zhou, Peng Chen, Zhiqiang Yu, Hui Zhang, Binqi Yang, Xingdong Pang, Mei Jiang, Yujian Cheng, Mustafa K. Taher Al-Nuaimi, Yan Zhang, Jixin Chen, and Shiwen He, "Multibeam antenna technologies for 5G wireless communications," *IEEE Trans. Antennas Propag.*, vol. 65, no. 12, pp. 6231-6249, Dec. 2017.
- [31] Roi Méndez-Rail, Cristian Rusu, Nuria Gonzlez-Prelcic, Ahmed Alkhateeb, and Robert W. Heath, "Hybrid MIMO architectures for millimeter wave communications: Phase shifters or switches?", *IEEE Access*, vol. 4, pp. 247-267, Jan. 2016.
- [32] Kraemer Michael , Dragomirescu Daniela , and Plana Robert, "Design of a very low-power, low-cost 60 GHz receiver front-end implemented in 65 nm CMOS technology," *Int. J. Microw. Wireless Technol.*, vol. 3, pp. 131-138, Apr. 2011.
- [33] Yikun Yu, Peter G. M. Baltus, Anton de Graauw, Edwin van der Heijden, Cicerio S. Vaucher, and Arthur H. M. van Roermund, "A 60 GHz phase shifter integrated with LNA and PA in 65 nm CMOS for phased array systems," *IEEE J. Solid-State Circuits*, vol. 45, no. 9, pp. 1697-709, Sep. 2010.
- [34] Shuguang Cui, Andrea J. Goldsmith, and Ahmad Bahai, "Energy-efficiency of MIMO and cooperative MIMO techniques in sensor networks," *IEEE J. Sel. Areas Commun.*, vol. 22, no. 6, pp. 1089-1098, Aug. 2004.
- [35] K. Satyanarayana, Mohammed El-Hajjar, Ping-Heng Kuo, Alain Mourad, and Lajos Hanzo, "Millimeter wave hybrid beamforming with DFT-MUB aided precoder codebook design," in *Proc. IEEE Veh. Technol. Conf. (VTC)*, Sep. 2017, pp. 1-5.